Russian Chemical Reviews **67** (10) 883 – 904 (1998) © 1998 Russian Academy of Sciences and Turpion Ltd

UDC 546.718

Physicochemical properties of technetium acido clusters

S V Kryutchkov

Contents

I.	Introduction	883
II.	Optical spectra of technetium clusters in the visible, UV, and IR spectral regions	883
III.	Magnetochemistry of technetium oxo and halide complexes	889
IV.	X-Ray photoelectron study of the structure of technetium complexes	894
V.	Chemical shifts in X-ray K_α emission spectra of technetium compounds	898
VI.	Compounds with ferrocenium cations	900
VII.	Conclusion	903

Abstract. The review is concerned with the electronic and molec ular structure and physicochemical properties of all types of technetium clusters with acido ligands described to date. As a typical cluster-forming metal, technetium possesses a number of specific, anomalous cluster-forming properties that can be interpreted in terms of greater capability of outer diffuse 5*s*(5*p*) AOs to participate in the formation of additional M—M bonds in technetium acido clusters as compared to analogous clusters of other transition *d*-elements. Theoretical interpretation of the electronic and molecular structure and properties of technetium clusters has been confirmed by experimental data (X-ray analysis, magnetochemistry, and EPR, optical, X-ray photoelectron and X-ray emission spectroscopy). The experimentally observed increased stability of technetium clusters with odd numbers of 'metallic' electrons and a decrease in the effective charge on Tc atoms upon formation of the M—M bonds are discussed. Recently found 'anomalous' properties of technetium and rhenium compounds with ferrocenium cations (in particular, unusual low-temperature electron emission on X-ray irradiation) are also considered. The bibliography includes 101 references.

I. Introduction

Compounds with metal – metal bonds (clusters) were first isolated and structurally characterised early in the 1960s. Several thousands of clusters are known to date.[1] Among all compounds of transition elements belonging to this type, only about 80 technetium-containing clusters with acido ligands have been described.[2] This is mainly due to difficulties encountered in the synthesis of complexes of radioactive elements. However, a great interest has been expressed in such technetium clusters, because they possess a set of 'anomalous' structural and other physicochemical properties.[3] In the present review, generalisation of experimental data on the known technetium acido clusters† has been made with primary emphasis on studies of physicochemical characteristics of these compounds (optical spectra in the visible, UV, and IR regions, magnetochemistry, X-ray emission spectra, X-ray photoelectron spectra, ^{57}Fe Mössbauer spectra, electric conductivity and other properties) and comparison with those of mononuclear technetium complexes. All fundamental physicochemical properties of technetium acido clusters insufficiently covered in previous reviews[1–3] are considered in particularly great detail.

All technetium acido clusters known to date have been systematised according to their electronic and molecular structure and to the method of their synthesis.[2] The nuclearity of the cluster, *i.e.*, the number of metal atoms forming direct metal – metal (M—M) bonds in the metal core of a cluster, is the basis of classification. In accordance with this principle, all technetium clusters are subdivided into di- and polynuclear clusters. Further classification is based on the electronic structure of the M—M bonds in the metal core of clusters and their molecular structure (*e.g.*, dinuclear d^4–d^4 clusters of the 'lantern' structural type or trigonal-prismatic hexanuclear clusters with metal – metal bonds of high order). The main structural types of technetium clusters are shown schematically in Fig. 1. The most important physicochemical properties of these clusters will be considered below.

II. Optical spectra of technetium clusters in the visible, UV, and IR spectral regions

1. Electronic spectra

No information on systematic studies of the optical spectra of technetium clusters has been reported to date. At best, spectral parameters of particular compounds were reported, and their qualitative assignment was made by analogy, *e.g.*, with rhenium compounds.[4–7] This is first of all due to difficulties in recording and interpreting the spectra, since this requires rigorous quantum-chemical calculations and precise spectroscopic measurements on single crystals in polarised light. The most precise spectroscopic studies have been carried out only for two clusters, *viz.*, $K_3[Tc_2Cl_8]\cdot 2H_2O$[8] for which scattered-wave self-consistent field (SCF – X_α-SW) quantum-chemical calculations[9] have been performed, and for $[Tc_2(2\text{-PyO})_4Cl]$ (where 2-PyO is the 2-hydroxypyridine alcoholate)[10] for which it has been possible to obtain suitable single crystals with all molecules oriented along the *z* axis of the tetragonal unit cell. The results of these studies have been described in detail;[1] therefore, it is hardly reasonable to repeat

S V Kryutchkov Institute of Physical Chemistry, Russian Academy of Sciences, Leninskii prosp. 31, 117915 Moscow, Russian Federation. Fax (7-095) 335 17 78. Tel. (7-095) 335 20 04

Received 16 October 1997
Uspekhi Khimii **67** (10) 969 – 992 (1998); translated by A M Raevsky

† Here, we are dealing with compounds with metal – metal chemical bonds and weak crystal field ligands that are anions of mineral acids: Cl^-, Br^-, I^-, SO_4^{2-}, *etc.*

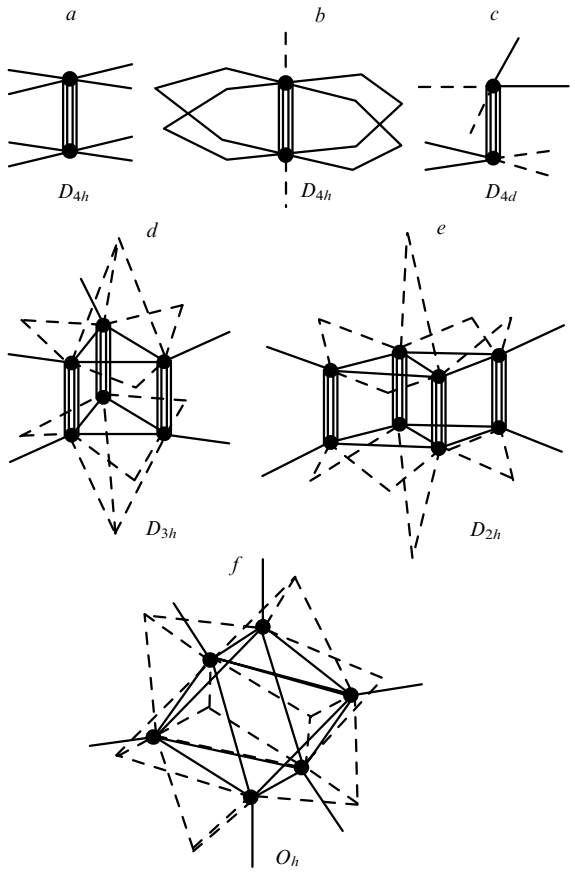


Figure 1. The main structural types of technetium acido clusters:[2] (*a*) $[Tc_2X_8]^{n-}$ (X = Cl, Br; n = 2, 3); (*b*) $\{[Tc_2L_4]X_m\}^{n-}$ (L = SO_4^{2-}, AcO^-, Bu^tCOO^-, 2-PyO$^-$; X = Cl, Br, H_2O, m = 1, 2; n = 0, 1, 2); (*c*) $[Tc_2X_6]^{2-}$ (X = Cl, Br); (*d*) $[Tc_6(\mu\text{-}X_6)X_6]^{n-}$ (X = Cl, Br; n = 0, 1, 2); (*e*) $[Tc_8(\mu\text{-}X_8)X_4]^{n-}$ (X = Br; n = 0, 1); and (*f*) $[Tc_6(\mu_3\text{-}Br)_5Br_6]^{2-}$. The positions of bridging or axial ligands are shown by dashed lines.

them in this review. We consider in brief only the most important conclusions drawn in these studies.

The optical spectra of the cluster $K_3[Tc_2Cl_8]\cdot 2H_2O$ in the region of the $\delta-\delta^*$ transition have been recorded at 300 and 3.7 K.[8] They belong to the lowest-energy electronic spectra. Fine structure associated with vibronic interaction and caused by progression in the ν'(M—M) frequency (320 cm^{-1} for the electronically excited state), *i.e.*, ν', $2\nu'$, $3\nu'$, *etc.*, is observed in these spectra. Since the M—M bond in the excited state is weaker than that in the ground state, the frequency ν' is about 50 cm^{-1} lower than the frequency of the ground electronic state ν(M—M). It should be noted that the ν(M—M) frequency is observed in the Raman spectra and is symmetry-forbidden in the IR spectra. The spectra of the $[Tc_2(2\text{-PyO})_4Cl]$ single crystal at 5 K in the region of the $\delta-\delta^*$ transition as well as in other regions appear to be much more complicated, since not only a progression based on the ν'(M—M) frequency (339 cm^{-1}), but also vibrations of the Tc—O and Tc—N bonds with frequencies ν_2', and ν_3' (264 and 298 cm^{-1}, respectively) are observed.[10] Thus, the O—O band is followed by peaks corresponding to the ν_1', ν_2' and ν_3' frequencies. Moreover, not only the expected extension of progressions to all possible overtones of frequencies ν_1' and ν_2', but also progressions based on combination frequencies are observed in the spectra. Thus, Cotton *et al.*[10] have identified vibrations with frequencies $5\nu_2'$, $4\nu_2' + \nu_1'$, $3\nu_2' + \nu_1'$, $2\nu_2' + 3\nu_1'$, $2\nu_2' + 4\nu_1'$, and $5\nu_1'$ in the fifth group of peaks (see also Ref. 8).

Electronic absorption spectra of solutions of potassium octachloroditechnetate in hydrochloric acid in the UV and visible regions have been studied,[4, 11] and the results (the dependence of the extinction coefficients ε_{max} on the HCl concentration) are listed in Table 1. As can be seen, the HCl concentration affects strongly the positions of the lines and the extinction coefficient in spectra of octachloroditechnetate ions, which is due to additional complexation and hydrolysis (see below).

Table 1. Dependence of the extinction coefficients of $[Tc_2Cl_6]^{3-}$ on the HCl concentration.[4, 11]

[HCl] / mol litre^{-1}	λ_{max} / nm	$10^3\,\varepsilon_{max}$ / litre mol^{-1} cm^{-1}	λ_{max}, / nm	$10^3\,\varepsilon_{max}$ / litre mol^{-1} cm^{-1}
11.4	647	0.33	322	3.6
10.2	643	0.32	320	3.5
7.6	640	0.29	320	3.6
6.5	638	0.29	320	3.0
5.9	635	0.26	318	2.7
4.8	630	0.25	318	2.5
3.0	618	0.19	315	2.2

Table 2 presents the assignment of bands in the spectra of $K_3[Tc_2Cl_8]\cdot 2H_2O$ and $[Tc_2(2\text{-PyO})_4Cl]$.[8, 10] An appreciably larger splitting between δ and δ^* MOs due to shortening of the Tc—Tc bonds in the oxopyridine complex is the major feature of the electronic spectra of these compounds.

Table 2. Electronic spectra of $[Tc_2Cl_8]^{3-}$ and $[Tc_2(2\text{-PyO})_4Cl]$ and the band assignment.[1, 8, 10]

$[Tc_2Cl_8]^{3-}$			$[Tc_2(2\text{-PyO})_4Cl]$		Transition
$10^3\,\nu_{max}$ / cm^{-1}	ε_{max} [a]	$10^3\,E_{calc}$ / cm^{-1}	$10^3\,\nu_{max}$ / cm^{-1}	I_{rel}	
5.9	630	6.0	13.0	m	$\delta-\delta^*$
13.6	35	15.8	18.0	vw, br	$\pi-\delta^*$
15.7	172	15.8	17.0	w, br	$\delta^*-\pi^*$
20.0	10	17.7	—	—	$\delta^*-d_{x^2-y^2}$
		20.2			$\delta^*-\sigma^*$
		21.3			$\delta-\pi^*$
		23.0			$\delta-d_{x^2-y^2}$
31.4	3900	28.3	25.0	s	LMCT
		29.1			LMCT
		31.2			$\pi-\pi^*$
		32.5			$\pi-d_{x^2-y^2}$
37.2	5600	~42	—	—	LMCT
		~41			LMCT
		~44			LMCT

Note. E_{calc} is the calculated transition energy, I_{rel} is the relative intensity, and LMCT denotes the bands with ligand to metal charge transfer. The bands with electric dipole transitions are underlined.
[a] Measured in litre mol^{-1} cm^{-1}.

Selected parameters of the electronic absorption spectra of technetium clusters are listed in Table 3. These data are far from being complete and thus can be used mainly for qualitative analysis. It is likely that the only exception is the $\pi-\delta^*$ transition ($\lambda_{max} \approx 600-700$ nm) that can be identified for all d^4-d^5 complexes by analogy with the $[Tc_2Cl_8]^{3-}$ ions. The absorption bands of this optical transition correlate well with the quantity $10Dq$[4] characterising the strength of the crystal field of the ligand environment in the dinuclear complexes in question. It should be noted that an analogous tendency is also observed for most of other bands.

The electronic spectra of polynuclear technetium clusters are characterised by the absence of clearly defined absorption bands and by a monotonic increase in the optical density with increase

Table 3. Electronic absorption spectra of technetium clusters.

Cluster	λ_{max} / nm (ε_{max}[a] or I_{rel})	Note	Ref.
$[Tc_2(\mu\text{-}O)_2(H_2EDTA)_2]$	~500 (2000), ~600 (< 200)	aqueous solution	14
$[Tc_2(\mu\text{-}O)_2(H_2EDTA)_2]^-$	~610 (s)	ditto	14
$[Tc_2(\mu\text{-}O)_2(TCTA)_2]^{2-}$	~510 (s)	"	14
$[Tc_2(\mu\text{-}O)_2(TCTA)_2]^{3-}$	592 (s)	"	14
$[Tc_2Cl_8]^{2-}$	~680 (w), 391 (m), 303 (m), 238 (s)	TBA salt in CsCl pellet at 10 K	5
$[Tc_2Cl_8]^{3-}$	676 (w), 388 (w, sh) 337 (m), 308 (w, sh)	ditto	5
$[Tc_2I_8]^{3-}$	760 (~250)	solution in HI (conc.)	4
$[Tc_2Br_8]^{3-}$	690 (400)	solution in HBr (conc.)	15
$[Tc_2(AcO)_4Cl_2]^{2-}$	620 (~200)	solution in AcOH	4
$[Tc_2(SO_4)_4]^{2-}$	700 (~300)	solution in H_2SO_4	16
$[Tc_2Cl_6]^{2-}$	460 (~600)	solution in HCl	4
$[Tc_2Br_6]^{2-}$	~480 (~600)	solution in HBr	4

Note. TBA is tetra-n-butylammonium, EDTA is ethylenediaminetetraacetate and TCTA is 1,4,7-triazacyclononane triacetate.
[a] Measured in litre mol^{-1} cm^{-1}.

in energy.[4] This is due to a large number of allowed electronic and vibronic transitions close in energy in the molecules of these compounds, which precludes their experimental observation because of limited resolution of spectrometers.

Despite the small number of reliable theoretical assignments of electronic spectra of technetium clusters, they are successfully employed by experimentalists, *e.g.*, in studies of the mechanism and kinetics of reactions in solutions.[2, 4, 11, 15, 17] Typical changes in the absorption spectra of potassium octachloroditechnetate in hydrochloric acid solutions in the presence and in the absence of atmospheric oxygen are shown in Fig. 2. Based on these data, the kinetics and mechanisms of acid hydrolysis, complexation, disproportionation with the cleavage of M—M bonds, oxidative addition of atmospheric oxygen to a multiple M—M bond and cycloaddition of multiple M—M bonds with the formation of polynuclear clusters occurring in the system under consideration and characterising the stability of octahalotechnetate ions in solutions of hydrohalogenic acids have been studied. Each reaction dominates under particular conditions depending on the chemical nature of the solvent, concentration of dinuclear complexes and complexing agent, temperature, *etc*. Based on kinetic experiments on the stability of octahaloditechnetate ions in solutions of hydrohalogenic acids, it has been possible to calculate the effective rate constants for some of the reactions listed above and, in particular, to establish that the stability of these ions in solutions and their thermal stability in the solid state is determined by the strength of the M—M bonds and decreases in the series Cl > Br > I.[2]

2. Vibrational spectra

The vibrational spectra of technetium clusters have been studied somewhat more thoroughly. However, most of them are not very informative, since the fundamental vibrational modes of cluster fragments themselves are observed in the long-wave region. Moreover, the most interesting ν(M—M) vibrations are forbidden in the IR spectra due to the centrosymmetric structure of most of the clusters and are allowed in the Raman spectra that cannot be

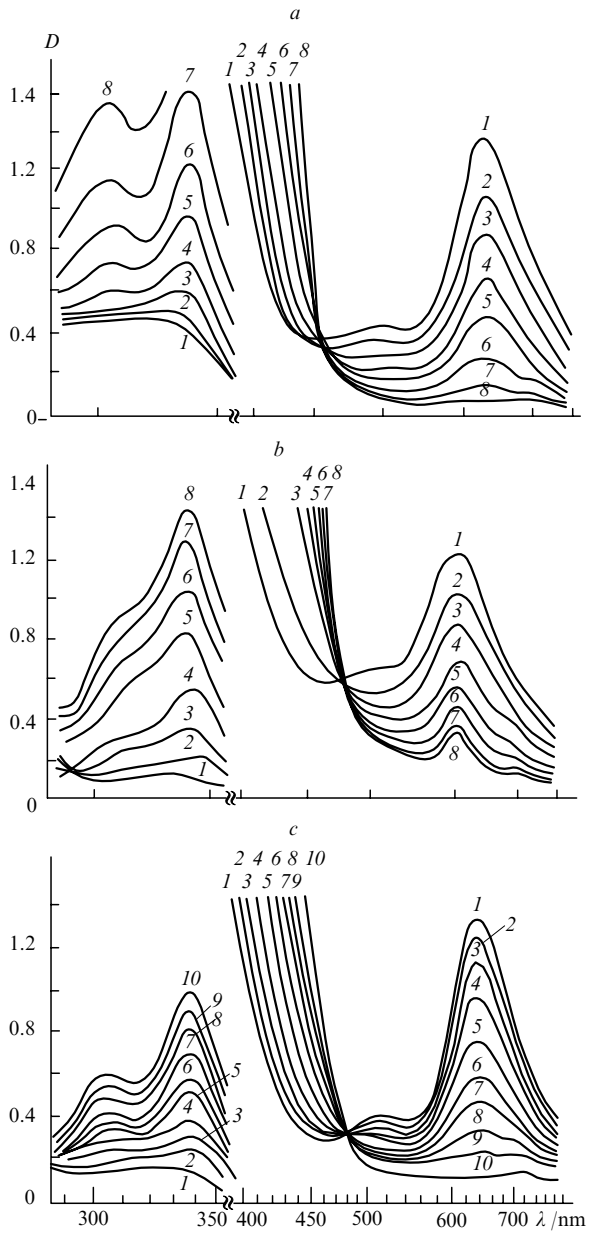


Figure 2. Typical changes in the absorption spectra of solutions of $K_3[Tc_2Cl_8]\cdot H_2O$ in hydrochloric acid in the absence (*a*) and in the presence of atmospheric oxygen (*b*, *c*) at initial concentrations of octachloroditechnetate(II, III) ions of less than 5×10^{-4} mol litre^{-1} (*a*, *b*) and more than 5×10^{-3} mol litre^{-1} (*c*). The duration of the oxidation of $[Tc_2Cl_8]^{3-}$ with oxygen (*b*, *c*) and of disproportionation of $[Tc_2Cl_8]^{3-}$ (*a*) increases uniformly in the order of increasing the numbers of spectra in the series (*1 – 10*).[4, 17]

recorded in many cases because of an intense dark colour of the compounds. Thus, only the IR spectra containing bands corresponding to stretching and bending vibrations of the atoms in cations or to characteristic vibrations of the Tc—X bonds (X is a ligand) can be observed for most of the technetium clusters. In this case, the Tc—X type of vibrations can be isolated from a set of more complex normal vibrations only by convention, since these can hardly be considered as characteristic ones because of large masses and strong mutual influence of the ligands. As has been mentioned in the previous Section, vibronic spectra can serve as yet another source of information on the cluster vibrational modes. However, vibrational progressions observed in this case will be characteristic of the electronically excited state of the cluster rather than of its ground state.[18]

Table 4. Frequencies and relative intensities of the bands of bending (δ) and stretching (ν) vibrations of OH groups in the IR spectra of technetium clusters (in KBr pellets).[19]

Compound	δ(H—OH) / cm^{-1}			ν(OH) / cm^{-1}	
	$\delta(H-OH)_{H_3O^+}$	δ(HO—μ-H)	$\delta(H-OH)_{H_2O}$	H_3O^+	H_2O
$\{[Tc_8(\mu\text{-}Br)_8Br_4]Br\}\cdot 2H_2O$ (**1**)	—	—	1620 (m)	—	3520 (br, s)
$[H(H_2O)_2]\{[Tc_8(\mu\text{-}Br)_8Br_4]Br\}$ (**2**)	1030 (w)	1410 (m)	1620 (m)	3150 (vw)	3540 (br, s)
$[H(H_2O)_2]_2\{[Tc_8(\mu\text{-}Br)_8Br_4]Br_2\}$ (**3**)	1040 (m)	1420 (m)	1620 (m)	—	3550 (br, s)
$[H_3O(H_2O)_3]_2[Tc_6(\mu_3\text{-}Br)_5Br_6]$ (**4**)	1045 (m)	1400 (m)	1618 (m)	—	3550 (br, s)
$[H_3O(H_2O)_3]_2[Tc_6(\mu_3\text{-}Br)_5Br_6]\cdot 4H_2O$ (**5**)	1035 (m)	1420 (s)	1620 (s)	—	3550 (br, s)
$[H_3O(H_2O)_3]_2[Tc_6(\mu_3\text{-}Br)_5Br_6]\cdot nH_2O$ (**6**) [a]	980 (s)	1322 (m)	1390 (m)	—	2800 (vw)
	1040 (s)	1350 (m)	1620 (s)	—	2930 (w)
		1420 (s)			3020 (w)
$(H_3O)_2[TcBr_6]$ (**7**)	1030 (m)	—	—	3150 (m)	
$K'_{3-x}K''_6(H_3O)_x[Tc_2Cl_8]_3\cdot nH_2O$ (**8**) [b]	—	—	1610 (m)	2965 (w)	3550 (br, s)
				2930 (w)	
				2865 (w)	

[a] Partially deuterated specimen. [b] K′ denotes K^+ ions in special three-fold position in the structure (on the two-fold axis) and K″ denotes K^+ ions in general position in the structure.

Thus, all available information on the vibrational spectra of technetium clusters is reduced mainly to characteristic atomic vibrations in the cations in the region 4000 – 400 cm^{-1} and to vibrations of cluster anions (or molecules) themselves in the region 400 – 50 cm^{-1}. Since the anions of different chemical nature have little effect on the cations, the absorption bands corresponding to characteristic vibrations of the same cations in different compounds differ insignificantly in most of spectra. In this connection, the IR spectra in the region 4000 – 400 cm^{-1} can be used mainly for qualitative analysis, and it makes no sense to consider them in this review, since they are rather characteristic of the cations themselves. Apparently, the IR spectra of differently hydrated hydroxonium cations and certain bridging bidentate (*e.g.*, carboxylate or sulfate) ligands are the exceptions, since they can contain essential information on the formal charge and on the electronic and molecular structure of the cluster fragments. Let us consider the results obtained from these spectra in more detail.

The absorption bands corresponding to stretching and bending vibrations of the OH groups in technetium clusters with differently hydrated hydroxonium cations[19] are listed in Table 4. The results obtained indicate that the pattern of the IR spectra depends on the character of bonding of the OH groups in crystals of the compounds in question. For instance, since only isolated H_3O^+ ions are present in the crystals of compound **7**, only two bands corresponding to the $\nu(OH)_{H_3O^+}$ and $\delta(H-O-H)_{H_3O^+}$ vibrations are observed in its IR spectrum (see Table 4). Only water molecules of crystallisation are present in the cluster **1**; therefore, only absorption bands due to the $\nu(OH)_{H_2O}$ and $\delta(H-O-H)_{H_2O}$ vibrations are observed in the IR spectrum of this compound. As can be seen, their positions differ considerably from those of corresponding absorption bands of hydroxonium cations.

Several bands due to stretching and bending vibrations of the OH groups are simultaneously observed in the IR spectra of compounds **2** – **5** and **8** (see Table 4). This is probably due to the fact that the bridging hydrogen atoms in the $[H(H_2O)_2]^+$ and $[H_3O(H_2O)_3]^+$ cations are closer to one of the oxygen atoms while to the other oxygen atom they are bonded by a strong hydrogen bond. Therefore, the absorption bands corresponding to vibrations of both H_3O^+ ions and H_2O must be observed in the IR spectra of hydrated hydroxonium cations. It should be noted that in this case the frequencies of δ(H—O—μ-H) absorption bands must be intermediate between those of the $\delta(H-O-H)_{H_2O}$ and $\delta(H-O-H)_{H_3O^+}$ vibrations. A much larger number of bands corresponding to bending vibrations must be observed in the case of partially deuterated differently hydrated hydroxonium ions (see Table 4). Thus, IR spectra, as well as the experiments on thermal dehydration and magnetic measurements, can be used to establish[19] the structure of clusters if their crystals contain differently hydrated hydroxonium cations, whereas X-ray analysis provides no unambiguous solution of this problem. Yet another example of this type is provided by the IR spectra of compound $(Bu^n_4N)_2[Tc_6(\mu_3\text{-}Br)_5Br_6]$ in which no absorption bands corresponding to vibrations of the OH groups are observed. In contrast to the initial assumptions,[20] this indicates that the $[Tc_6(\mu_3\text{-}Br)_5Br_6]^{2-}$ anion contains no OH groups.

The IR spectra of μ-acetato dinuclear d^4–d^5 technetium complexes have been studied and all absorption bands have been assigned.[21] Previously,[7] the IR spectra of analogous dinuclear d^4–d^4 technetium and rhenium clusters have been studied; however, no complete assignment of the absorption bands has been performed. From comparison of the results obtained it follows that, in contrast to analogous dinuclear complexes of other elements (*e.g.*, copper acetates), the splitting (Δ) between the frequencies of symmetric ν_s(C—O) and antisymmetric ν_{as}(C—O) vibrations of the bridging acetate anions in technetium clusters is extremely small ($\sim$ 20 cm^{-1}). It should be noted that a tendency for the Δ value to decrease is observed on going from monodentate acetate ions to bidentate ones and that the anomalously small value of this splitting is probably due to a specific influence of strong Tc—Tc bonds. The frequencies of the ν(Tc—X) vibrations are appreciably shifted towards the long-wave region relative to analogous frequencies of other halide technetium complexes without bridging ligands. This indicates appreciable weakening of the Tc—X bonds in μ-acetato technetium complexes as compared to analogous bonds in other halide Tc complexes (Table 5). From these data altogether it has been suggested[21] that the compounds under consideration have the 'lantern' type of structure (see Fig. 1 *b*), *viz.*, two technetium atoms form a strong Tc—Tc bond, four bridging acetate ions additionally bind Tc atoms to one another, while two halide ions are in axial positions with respect to the M—M bonds and are in essence ionically bonded to the technetium atom. This assumption has been completely confirmed by X-ray analysis.[22–24]

Using the IR spectra, the structures of sulfate dinuclear technetium complexes have also been determined.[16] The parameters of the IR spectra and the assignment of bands of two sulfate dinuclear technetium complexes, $K_2[Tc_2(SO_4)_2]\cdot 2H_2O$ and $K_4(H_3O)_2[Tc_2(SO_4)_6]$, are listed in Table 6. The IR spectrum of the former compound contains absorption bands in the region 330 – 3530 cm^{-1} with maxima at 3450 and 1655 cm^{-1} corresponding to stretching and bending vibrations of coordinated water molecules, respectively. Four groups of bands each split by the crystal field are observed in the regions of both stretching and

Table 5. Frequencies of absorption bands (cm^{-1}) in the long-wave IR spectra of technetium halide clusters and their assignment.[28,29]

Cluster	ν(M—M),	ν(M—X),	δ(XMY), δ(MMX)
$[Tc_2(AcO)_4Cl]$	—	~180	—
$[Tc_2(AcO)_4Br]$	—	~120	—
$[Tc_2(2\text{-}PyO)_4Cl]$	383 [a] (337 [b]) [10]	—	—
$[Tc_2Cl_8]^{2-}$	—	362, 342	179, 170
$[Tc_2Br_8]^{2-}$	323 [a 5]	269, 249 [5]	—
$[Tc_2Cl_8]^{3-}$	370 [a] (320 [b]) [1]	335, 310	184, 157
$[Tc_2Cl_6]_n^{2n-}$	—	~310, 285	183, 175
$[Tc_6Br_{12}]$ (see [c])	324, 302, 298	234, 170	141, 120. 106
$[Tc_6Br_{12}]^-$ (see [c])	349, 335, 298	230, 181	~100
$[Tc_6Cl_{12}]^-$ (see [c])	349, 336, 298	253, 233	189, 176, 153, 122
$[Tc_6Cl_{12}]^{2-}$	~360 (br)	~303 (br) ~254 (br)	195, 153
$[Tc_8Br_{12}]$ (see [c])	355, 290, 266	232, 213	120, 96
$[Tc_8I_{12}]$ (see [c])	342, 283, 243	187, 113	80, 61, 54
$[Tc_6Br_{11}]^{2-}$	330, 292	266, 238 (w)	164 (w), 120, 76

[a] Data of Raman spectra. [b] Data of vibronic spectra. [c] Axial ligands are omitted.

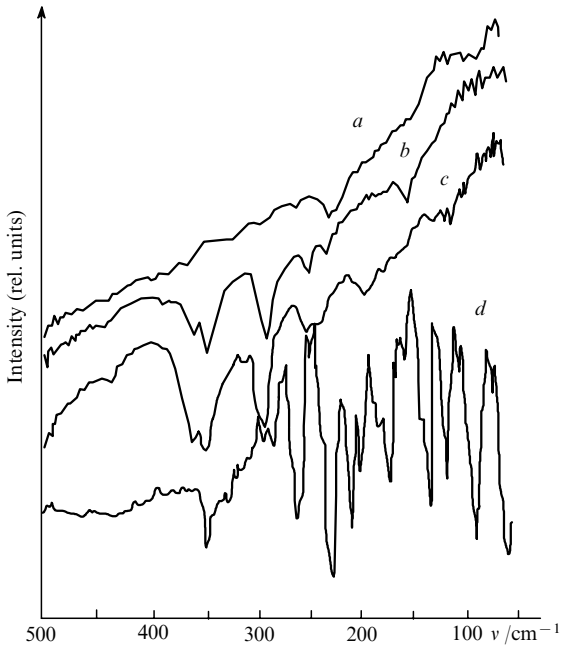


Figure 3. The long-wave IR spectra of polynuclear technetium clusters:[28,29] (*a*) $(FeCp_2)_2[Tc_8Br_{14}]$; (*b*) $(FeCp_2)_3[Tc_6Cl_{14}]$; (*c*) $(Bu^n_4N)_3.[Tc_6Cl_{14}]$; and (*d*) $[H(H_2O)_2]_2[Tc_8Br_{14}]$.

bending vibrations of sulfate ions; this corresponds to distortion of the tetrahedral SO_4^{2-} ion to the idealised C_{2v} symmetry due to the formation of bidentate bridging bonds between the sulfate ions and the Tc_2^{6+} fragment,[25] which is analogous to those found in the structure of the $[Re_2(SO_4)_4]^{2-}$ anion.[26,27]

The IR spectrum of compound $K_4(H_3O)_2[Tc_2(SO_4)_6]$ is characterised by a more intense absorption band in the region ~ 2950 cm^{-1}, which can be assigned to the $\nu(OH)_{H_3O^+}$ vibrations (see Table 6). Three groups of broad bands are observed in the region of stretching and bending vibrations of the S—O bond in the spectrum of this compound; this is characteristic of monodentate sulfate ions with C_{3v} symmetry.[25]

Later, the assumptions [16] concerning the structure of compound $K_2[Tc_2(SO_4)_4]\cdot 2H_2O$ made on the basis of IR spectra, the results of chemical analysis and data of thermogravimetric analysis and other physicochemical methods were confirmed by X-ray study of a single crystal synthesised by the author of this review.‡

The assignment of the absorption bands of a number of di- and poly-nuclear halide technetium clusters is given in Table 5 and the long-wave IR spectra of several polynuclear technetium clusters are shown in Fig. 3. The following major tendencies are observed for compounds of similar structure, *viz*., the absorption bands corresponding to the ν(Tc—X) and δ(Tc—Tc—X) vibrations are, as a rule, shifted towards the low-energy region as the formal oxidation state of technetium decreases and the replacement of ligands in the series Cl, Br and I occurs. As has already been noted, vibrations of the M—M bonds are symmetry-forbidden and are not observed in the IR spectra of most of dinuclear clusters; however, in polynuclear clusters this exclusion is removed, and certain ν(Tc—Tc) and δ(Tc—Tc—X) vibrations can also be observed in the IR spectra. Thus, the stretching vibrations of the M—M bonds of F_{1u}; E' and A''; and B_{1u}, B_{2u} and B_{3u} symmetry types are expected to be observed in the spectra of octahedral, trigonal-prismatic, and tetragonal-prismatic clusters, respectively. For lack of sufficient experimental data, unambiguous assignment of all vibrational frequencies for polynuclear clusters is currently impossible. Therefore, their long-wave IR spectra can be used mainly for qualitative analysis and determination of the structure. Thus, a large number of relatively narrow absorption bands in this spectral region is almost unambiguous evidence for the polynuclear nature of the clusters, while the positions of these lines can be tentative evidence for the formal oxidation state of technetium.

The use of IR spectra of technetium and rhenium complexes with ferrocenium cations for the solution of analytical and structural problems has been described.[28,29] The composition

‡ X-Ray analysis has been done by P A Koz'min, M D Surazhskaya, and T B Larin and the results of these investigations have been described in Ref. 2.

Table 6. Frequencies (cm^{-1}) and relative intensities of bands in the IR spectra of sulfate dinuclear technetium complexes.[16]

Compound	ν(OH)	δ(H—O—H)	ν(S—O)	ν(Tc—O)	δ(O—S—O)	Other bands
$K_2[Tc_2(SO_4)_4]\cdot 2H_2O$ [a]	3450 (s, br)	1655 (w)	1295 (s), 1230 (w); 1185 (sh), 1155 (s); 1070 (m), 1041 (m); 915 (s), 850 (m)	698 (m)	698 (s); 600 (m), 585 (m); 532 (sh, w), 522 (w); 465 (m)	381 (m), 335 (s, br) δ(O—Tc—O), 250 (sh, br), 200 (m), 181 (w), 158 (m), 152 (w), 118 (m), 78 (s)
$K_4(H_3O)_2[Tc_2(SO_4)_6]$ [b]	2950 (sh, br)		1230 (sh, br), 1155 (s); 1045 (s); 965 (s), 850 (sh)	675 (m)	605 (s); 535 (w); 483 (m)	290 (s, v br) δ(O—Tc—O) 156 (s, v br), 80 (w, br)

[a] Sulfate ions have C_{2v} symmetry in the complex $K_2[Tc_2(SO_4)_4]\cdot 2H_2O$. [b] Sulfate ions have the C_{3v} symmetry in the complex $K_4(H_3O)_2[Tc_2(SO_4)_6]$.

and structure of these complexes suggest that the lines corresponding to vibrations of ferrocenium cations, technetium or rhenium anions, and hydrated hydroxonium cations {in the case of compound $(FeCp_2)_4[H_3O(H_2O)_4]_2\cdot[TcCl_6]_3$} must be observed in their IR spectra. According to the published data,[30] if ferrocene and ferrocenium have the $D_{5d}(D_{5h})$ point symmetry, then vibrations of $A_{2u}(A_2'')$ and $E_{2u}(E_2'')$ symmetry types must be active in their IR spectra. It has been shown [28,29] that all most intense vibrational lines of ferrocene are also observed in the IR spectra of technetium and rhenium compounds with ferrocenium cations. The only exception are the absorption bands in the region 480–820 cm^{-1}, where only one composite line in the region 670–560 cm^{-1} is observed instead of very intense bands corresponding to the nonplanar ρ_{CH} (A_{2u}) vibrations and $\nu(Fe-Cp)$ (E_{1u}) stretching vibrations characteristic of pure ferrocene; this line is probably due to the interaction between the above two vibrations. It is known [30] that interaction between these types of vibrations [as well as a shift of $\nu(Fe-Cp)$ towards the high-frequency region] characterises an increase in covalency of the Fe–Cp bonds. It should be noted that neither absorption bands corresponding to the $\nu(Fe-Cp)$ (E_{1u}) vibrations in the IR spectrum of compound $(FeCp_2)_2[Tc_8Br_{14}]$ nor the bands corresponding to bending skeletal $\nu(Cp-Fe-Cp)$ (E_{1u}) vibrations in the spectra of all compounds studied are observed. All bands in the IR spectra of compounds containing $[Tc_6Cl_{14}]^{3-}$ and especially $[Tc_8Br_{14}]^{2-}$ anions are considerably broadened and diffuse (see Fig. 3). Analogous effects have been found for certain specimens preliminarily frozen to $\sim$ 78 K. It has been pointed out that this phenomenon can be due to the effects of vibronic interaction in the molecules.[29,30]

As to the absorption bands corresponding to stretching and bending vibrations of isolated hydroxonium cations in the cluster $[Fc(Cp_2)]_4[H_3O(H_2O)_4]_2[TcCl_6]_3$, it is difficult to identify them because of the superposition of more intense lines of ferrocenium cations. Nevertheless, certain bands in the region of $\delta(H-O-H)$ bending vibrations (at 1620, 1555, 1510, and 1058 cm^{-1}) can be identified unambiguously. The conclusion that the effect of ferrocenium cations on the vibrational spectra of anions is not so significant as the reverse effect of various anions on the vibrations in ferrocenium cations is yet another important result.[28,29] Nevertheless, this effect persists and manifests itself mainly as a shift of frequencies of these vibrations. Similar shift of the frequencies of stretching and bending vibrations of technetium anions due to the effect of various cations has been found;[31] it has been shown that the absorption bands of the anions are shifted towards the low-frequency region as the average size of cations increases. For pertechnetate ions, an increase in the cation size is accompanied by a decrease in the splitting of the $\nu(Tc=O)$ stretching band. Comparison of published data (see Refs 28, 29 and 31) shows that the extent to which the anions are affected by the ferrocenium cations, the effective radius (R_{eff}) of which is larger than 3 Å, approaches that of $(Me_4N)^+$ and $(Et)_4N^+$ having similar R_{eff}. It should be noted that the absorption bands in the long-wave IR spectra of compound $(FeCp_2)_2[Tc_8Br_{14}]$ are also considerably broadened and some of them are missing (see Fig. 3), as is the case of the short-wave IR spectra. This may also be associated with vibronic interactions.[28,29]

The IR spectroscopic studies of ferrocenium salts with Tc- and Re-containing anions [28,29] have shown that:

1. All compounds correspond to the expected composition and structure.

2. The absence of additional absorption bands in the IR spectra of the compounds obtained (except for the bands corresponding to anionic and cationic vibrations) indicates that no formation of new types of directed chemical bonds occurs except for those expected from the composition and structure of these compounds.

3. Strong mutual influence of the ferrocenium cations and the technetium (rhenium) anions is observed, which increases in the series of anions $[TcO_4]^- < [Re_2Br_8]^{2-} \approx [Tc_6I_{14}]^{3-} < [TcCl_6]^{2-} < [Tc_6Cl_{14}]^{3-} < [Tc_8Br_{14}]^{2-}$ and is probably due to the strengthening of vibronic interaction in this series.

The assignment of absorption bands in the long-wave IR spectra of $[Tc_2X_8]^{n-}$ (X = Cl, Br; n = 2, 3) dinuclear technetium clusters with a simpler structure has been performed.[1,4,5,8,32] Thus, the IR spectra of these anions contain two absorption bands with E_u and A_{2u} symmetry corresponding to the $\nu(Tc-X)$ stretching vibrations and one A_{2u} band corresponding to the $\delta(X-Tc-X)$ vibrations, while their Raman spectra contain two absorption bands with A_{1g} symmetry corresponding to the $\nu(Tc-Tc)$ and $\nu(Tc-X)$ vibrations and one band with E_g symmetry. The frequencies of these bands in the spectra of different anions are listed in Table 5.

Complete normal coordinate analysis for the $[Tc_2X_8]^{n-}$ dinuclear complexes (X = Cl, Br; n = 2, 3) has been performed, the bands in their IR and Raman spectra (including those of isotope-substituted complexes) have been assigned, and ten force constants have been calculated.[6] The structural characteristics of these ions used in the calculations and the force constants obtained are listed in Table 7. The assignment of bands in the IR and Raman spectra of analogous rhenium and osmium dinuclear complexes with D_{4h} and D_{4d} symmetry, respectively, has also been performed.[6] The calculations reproduce well the major regularities expected from the data of X-ray studies. Thus, from Ref. 6 and the data in Table 7 it follows that for all the complexes in question the bond stretching force constants $f_d(M-M)$ and $f_d(M-X)$, as a rule, decrease as the ligands are replaced in the series F, Cl, Br and I and n increases. It should be noted that these

Table 7. Bond lengths (d /Å), bond angles (α /deg) and force constants (f /mdyn A^{-1}) for $[Tc_2X_8]^{n-}$ (X = Cl, Br; n = 2, 3) ions.[6]

Parameter	$[Tc_2Cl_8]^{2-}$	$[Tc_2Cl_8]^{3-}$	$[Tc_2Br_8]^{2-}$	$[Tc_2Br_8]^{3-}$
$d(Tc-Tc)$	2.15	2.11	2.15	2.13
$d(Tc-X)$	2.32	2.36	2.47	2.51
$\alpha(Tc-Tc-X)$	103.80	104.60	103.90	104.00
$f_d(Tc-Tc)$	3.79	4.86	2.67	3.15
$f_d(Tc-X)$	1.79	1.47	1.48	1.31
$d^2(X-Tc)f_\alpha(X-Tc-X)$	0.67	0.64	1.55	1.60
$d(X-Tc)\,d(Tc-Tc)f_\alpha(X-Tc-Tc)$	1.09	0.88	1.37	1.15
$f_{dd}(TcTc-TcX)$	0.11	0.24	0.05	0.13
$f_{dd}(TcX-TcX)$	0.42	0.40	0.32	0.36
$d(Tc-X)f_{d\alpha}(TcX-XTcX)$	0.03	0.02	0.02	0.01
$d(Tc-X)f_{d\alpha}(TcTc-XTcTc)$	0.30	0.30	0.17	0.19
$d(Tc-X)\,d(Tc-Tc)f_{\alpha\alpha}(XTcTc-XTcTc)$	0.25	0.15	0.23	0.05

Note. The subscripts d and α at the force constants f correspond to stretching and bending vibrations, respectively; the direction of the vibrations is given in parentheses.

changes and changes in analogous interatomic distances due to ligand replacement and the decrease in the formal oxidation state of the metal occur in the opposite directions. Of all the complexes studied, the largest f_d(M—M) value was obtained for the $[Tc_2Cl_8]^{3-}$ anion with a formal M—M bond order of 3.5 for which the shortest M—M distance has been found experimentally.[2]

In conclusion of this Section, it should be noted that many problems associated with the assignment and interpretation of the optical spectra of technetium clusters remain unsolved due to the complex structure of these compounds, the lack of sufficient experimental data (which is often due to the impossibility of obtaining them with currently available instruments) as well as to the absence of reliable theoretical calculations. However, the available data can well be used for qualitative structural analysis.

III. Magnetochemistry of technetium oxo and halide complexes

Among experimental methods of studying the electronic structure of coordination compounds, magnetochemical measurements occupy a particular place since they make it possible to determine the number of unpaired electrons in the molecule, the magnitude of intermolecular exchange interactions, and in some instances can even serve as immediate evidence for the relative order of some MOs in the molecules of these compounds. Sometimes, magnetochemistry can be used as an analytical and, to some extent, as a structural investigation technique.[33] However, no information on systematic studies of magnetochemical properties of technetium complexes has been reported so far.[34] The results available[35,36] have not been systematised, contain no data on diamagnetic corrections for technetium and thus are unreliable. In connection with the foregoing, in this review we discuss the magnetic properties of technetium complexes in which Tc atoms have different oxidation states and which have been studied by the static magnetic susceptibility method and by EPR spectroscopy.

The data of magnetic measurements for technetium compounds are listed in Table 8. Since no diamagnetic corrections for technetium ions are known, they were obtained by extrapolating the data on diamagnetic corrections for neighbouring elements in the Periodic Table (Mn, Re, Mo and Ru).[34] The results of calculations of the electronic structure of technetium oxo and halide complexes are shown in Fig. 4. As can be seen, in most cases the experimental data are in good agreement with theoretical predictions. Let us consider the most typical cases in detail.

Pertechnetates are tetrahedral d^0 complexes. The recently found distortion of these complexes[37–44] has virtually no effect on their diamagnetic properties, except for weak temperature-

Table 8. Magnetic properties of technetium oxo and halide complexes.[18,28,34]

Compound	Tc oxidation state	Electron configuration	g_{eff}	μ_{eff}/μ_B		θ/deg	Number of unpaired electrons
				80 K	300 K		
$M[TcO_4]$ (M = K, NH_4, Bu^n_4N)	+7.0	d^0	—	see [a]	see [a]	—	0
$(FeCp_2)[TcO_4]$	+7.0	d^0	2.01	2.78	3.88	−185	1.95–3.00
$M_2[TcOCl_5]$ (M = K, NH_4)	+5.0	d^2	—	see [a]	see [a]	—	0
$(Bu^n_4N)[TcOX_4]$ (X = Cl, Br, I)	+5.0	d^2	—	see [a]	see [a]	—	0
$Tc_2O_5 \cdot nH_2O$	+5.0	d^2	—	see [a]	see [a]	—	0
$[TcO(NO_3)_3] \cdot H_2O$	+5.0	d^2	—	see [a]	see [a]	—	0
$K_3[Tc_2Cl_8O_2]$	+4.5	d^2-d^3	—	3.69	4.15	−40	3
$M_2[TcCl_6]$ (M = K, NH_4)	+4.0	d^3	—	2.79	3.44	−68	3
$1/3\ \{[FeCp_2]_4[H_3O(H_2O)_4]_2[TcCl_6]_3\}$	+4.0	d^3	2.015	6.94	6.80	9	6.02–5.87
$(Bu^n_4N)_2[TcCl_6]$	+4.0	d^3	—	3.78	3.80	0	3
$M_2[TcBr_6]$ (M = K, NH_4)	+4.0	d^3	—	3.21	3.45	−24	3
$M_2[TcI_6]$ (M = K, NH_4)	+4.0	d^3	—	2.79	3.34	−60	3
$(Me_4N)_2[TcI_6]$	+4.0	d^3	—	3.68	3.67	0	3
TcO_2	+4.0	d^3	—	~1.0	1.5	~200	~1
$(Bu^n_4N)_2[Tc_2X_8]$ (X = Cl, Br)	+3.0	d^4-d^4	—	see [b]	see [b]	—	0
$[Tc_2(RCOO)_4Cl_2]$ (R = Me, Bu^t)	+3.0	d^4-d^4	—	see [b]	see [b]	—	0
$K_2[Tc_2(SO_4)_4] \cdot 2H_2O$	+3.0	d^4-d^4	—	see [b]	see [b]	—	0
$M_3[Tc_2Cl_8] \cdot nH_2O$ (M = K, NH_4, C_5H_5NH, C_9H_8NH)	+2.5	d^4-d^5	2.09	1.75	1.75	0	1
$M_3[Tc_2Br_8] \cdot 2H_2O$ (M = K, NH_4)	+2.5	d^4-d^5	2.09	1.74	1.74	0	1
$[Tc_2(AcO)_4X]$ (X = Cl, Br)	+2.5	d^4-d^5	2.09	1.75	1.73	0	1
$K[Tc_2(AcO)_4Cl_2]$	+2.5	d^4-d^5	2.09	1.75	1.75	0	1
$1/2\ [Tc_4O_5] \cdot n\,H_2O$	+2.5	d^4-d^5	—	1.77	1.75	0	1
$M_2[Tc_2Cl_6]$ (M = K, NH_4; X = Cl, Br)	+2.0	d^5-d^5	—	see [b]	see [b]	—	0
$(Et_4N)_2\{[Tc_6(\mu\text{-}Br)_6Br_6]Br_2\}$	+2.0	$6d^5$	—	0.85	1.16	~0	~0.1
$M_3\{[Tc_6(\mu\text{-}X)_6X_6]X_2\}$ (X = Cl, Br, M = Me_4N, Bu^n_4N)	+1.83 (3)	$5d^5-d^6$	2.00 ($g_\parallel$), 1.63 ($g_\perp$)	~1.5	~1.7	~1	1
$(FeCp_2)_3\{[Tc_6(\mu\text{-}Cl)_6Cl_6]Cl_2\}$	+1.83 (3)	$5d^5-d^6$	2.007	5.75	6.01	~0	4.85–5.13
$(Bu^n_4N)_3\{[Tc_6(\mu\text{-}Cl)_6Cl_6]Cl_2\}$	+1.83 (3)	$5d^5-d^6$	2.00 ($g_\parallel$), 1.63 ($g_\perp$)	1.50	1.77	~0	1
$(Me_4N)_2[Tc_6(\mu\text{-}Cl)_6Cl_6]$	+1.66 (6)	$4d^5-2d^6$	1.97	~0.8	~1.1	−60	~0.2
$\{[Tc_8(\mu\text{-}Br)_8Br_4]Br\} \cdot 2H_2O$	+1.625	$5d^5-3d^6$	—	1.12	1.57	~120	1
$(Bu^n_4N)_3\{[Tc_6(\mu_3\text{-}Br)_5Br_6]$	+1.5	$3d^5-3d^6$	~2.0	0.73	0.91	~0	~0.1
$[H_3O(H_2O)_3]_2[Tc_6(\mu_3\text{-}Br)_5Br_6] \cdot nH_2O$ (n = 0, 4)	+1.5	$3d^5-3d^6$	~2.0	~1.0	~1.2	−80	~0.2
$[H(H_2O)_2]_n\{[Tc_8(\mu\text{-}Br)_8Br_4]Br_n\}$ (n = 1, 2)	+1.5	$4d^5-4d^6$	—	see [b]	see [b]	—	0
$(Bu^n_4N)_2\{[Tc_8(\mu\text{-}X)_8X_4]I_2\}$ (X = 0.5 Br + 0.5 I)	+1.5	$4d^5-4d^6$	—	see [b]	see [b]	—	0
$(FeCp_2)_2\{[Tc_8(\mu\text{-}Br)_8Br_4]Br_2\}$	+1.5	$4d^5-4d^6$	—	4.82	5.87	−64	3.83–4.96

[a] Compounds are diamagnetic. [b] Temperature-independent paramagnetism.

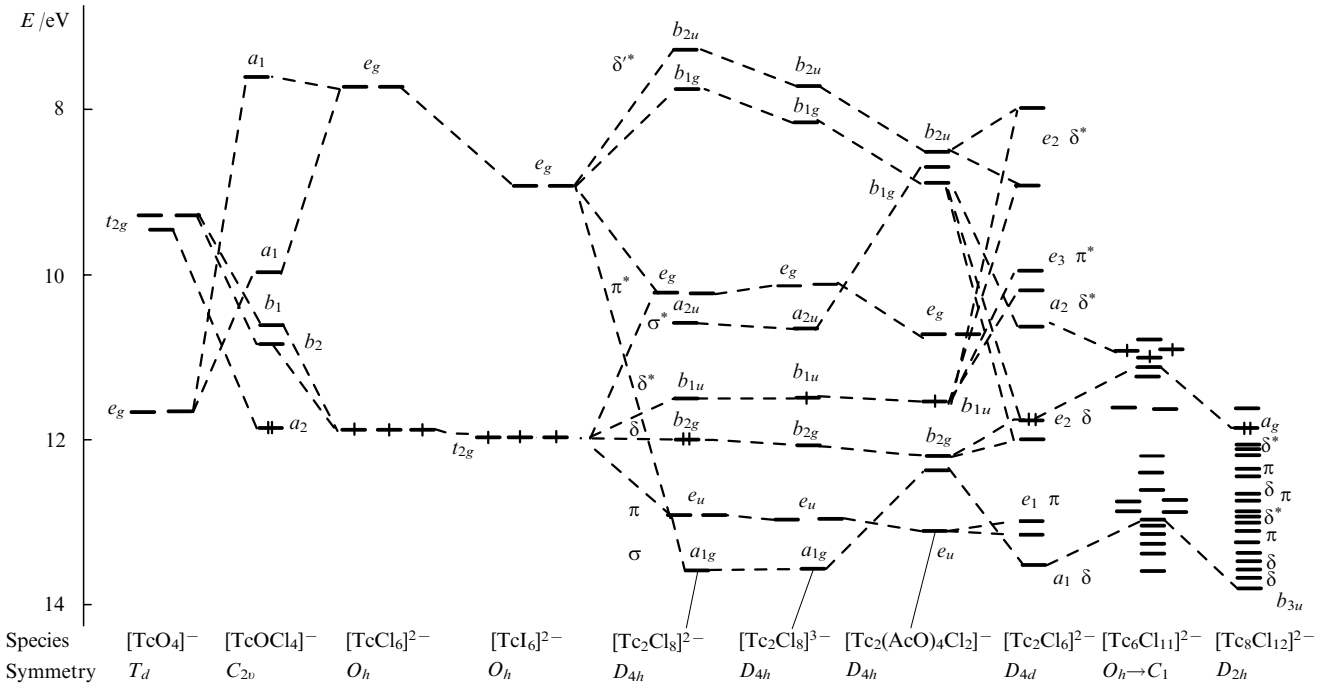


Figure 4. Results of extended Hückel (EH) calculations of the electronic structure of technetium complexes.[2, 34] The presence of electrons in the HOMO is depicted schematically by small double vertical lines.

independent paramagnetism (TIP)§ observed in some cases (see Table 8 and Fig. 4). It should be noted that according to Fig. 4, the $[TcO_4]^{2-}$ ions formed in the one-electron reduction of pertechnetates, must possess weak paramagnetism corresponding to one unpaired electron, which is observed experimentally.[45, 46]

Technetium(V) oxohalide complexes are characterised by the d^2 electronic configuration of the central atom. The ground electronic state of the molecules of these compounds must be spin-paired because of a symmetry breakdown in the nearest environment of technetium (*e.g.*, to C_{2v} for $[TcOX_4]^-$, see Ref. 47); in fact, these compounds also possess diamagnetism or TIP (see Table 8, Fig. 4).[34]

Technetium(IV) halide complexes are characterised by the d^3 electronic configuration and octahedral structure of the nearest coordination sphere of the Tc atoms. According to theoretical predictions (see Fig. 4), these compounds have a triply degenerate t_{2g} highest occupied molecular orbital (HOMO) and, hence, they must possess paramagnetism corresponding to the spin 3/2 ($\mu_{eff} \approx 3.87\ \mu_B$).

From the data in Table 8 it can be seen that only for several technetium(IV) compounds are the magnitudes of the effective magnetic moments μ_{eff} close to the pure spin value; in most cases, they are much smaller. Previously,[48] similar effects of a decrease in μ_{eff} of analogous rhenium halide complexes have been rationalised by intermolecular exchange interactions occurring along the $Re' - X' \cdots X'' - Re''$ chains. It has also been shown[48] that similar antiferromagnetic interactions can occur at $X' \cdots X''$ distances up to ~ 5 Å. Thus, antiferromagnetic exchange interactions in technetium(IV) complexes are also the most plausible explanation of the decrease in their effective magnetic moments.

In fact, as can be seen from the data in Table 8, a decrease in the size of the outer-sphere cation and an increase in the anion size (halide ion) leads to an increase (in the absolute value) in the Weiss constant characterising the strength of antiferromagnetic exchange interactions. However, in the case of rather bulky tetraalkylammonium cations, the $[TcX_6]^{2-}$ anions are 'pushed apart' by these cations to such an extent that the exchange interactions along the $Tc' - X' \cdots X'' - Tc''$ chains become impossible (the $X' \cdots X''$ distances between adjacent $[TcX_6]^{2-}$ octahedra are ~ 6 Å).[49] An even greater decrease in μ_{eff} is observed for technetium dioxide (see Table 8). According to the published data,[50] it is assumed that the metal–metal (Tc–Tc) bonds can be formed in the TcO_2 molecule; this may be an additional reason for the decrease in μ_{eff} compared to its pure spin value for technetium(IV).

As can be seen from the data in Table 8, the magnetic properties of most of the compounds considered above are first of all due to the electronic configuration of the Tc atoms, the symmetry of their nearest ligand environment and intermolecular exchange interactions. The magnetic properties of all other technetium compounds listed in Table 8 cannot be explained by these reasons only, since their electronic structures are strongly affected by the M–M bonds localised on pairs of Tc atoms or delocalised over the polynuclear metal core. In these complexes, the M–M interactions result in appreciable shortening of the Tc–Tc distances compared to analogous distances in compact metallic Tc.[1, 2, 51] The compounds studied[2, 51] can be divided into two structural types, *viz.*, dinuclear complexes (clusters) with multiple M–M bonds and polynuclear clusters.

Dinuclear d^4–d^4 complexes. Classical quadruple M–M bonds formed by $\sigma(4d_{z^2})$, $2\pi(4d_{xz}, 4d_{yz})$ and $\delta(4d_{xy})$ orbitals of the M–M bonds (see Fig. 4) are characteristic of these compounds.[1, 2, 51] These complexes have an eclipsed conformation of ligands (the idealised D_{4h} symmetry, see Fig. 1 *a,b*) and Tc–Tc distances in the range from 2.16 to 2.19 Å.[2] All compounds are characterised by the absence of unpaired electrons, therefore their magnetic susceptibility is temperature-independent (see Table 8).

Dinuclear d^4–d^5 complexes are formed as a result of one-electron reduction of the compounds belonging to the preceding group and also have an eclipsed conformation of ligands[1, 2, 51] (see Fig. 1 *a,b*). As could be expected from Fig. 4, one unpaired electron is shared by two Tc atoms that form an M–M bond of high order (the Tc–Tc distances in d^4–d^5 complexes lie within the limits 2.10–2.15 Å)[1, 2, 51] in the molecules of these compounds. It has been shown[3, 9, 52–54] that this electron occupies the b_{1u} HOMO (the δ* M–M orbital) formed mainly by the $4d_{xy}$

§ Unpublished results by K E German (Institute of Physical Chemistry, Russian Academy of Sciences).

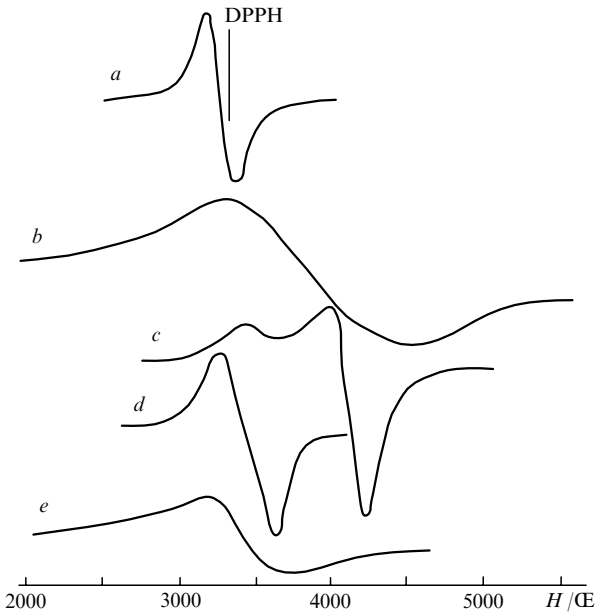


Figure 5. EPR spectra:[34] (*a*) $K_3[Tc_2Cl_8]\cdot 2H_2O$ at 78 K (the *z* crystal axis is perpendicular to the direction of the magnetic filed strength); (*b*, *c*) $(Me_4N)_3\{[Tc_6(\mu\text{-}Cl)_6Cl_6]Cl_2\}$ at 293 and 78 K; (*d*, *e*) $(Me_4N)_2.[Tc_6(\mu\text{-}Cl)_6Cl_6]$ at 78 and 293 K, respectively; DPPH is diphenylpicrylhydrazide.

orbitals of two technetium atoms. Thus, the M—M bonds in these complexes are of formal order 3.5. Let us present the essentials of this proof, since they are of importance for considering the electronic structure of the compounds mentioned.[2]

EPR signals of all compounds belonging to this type are observed both in the crystalline state and in solutions. Typical EPR spectra of $K_3[Tc_2Cl_8]\cdot 2H_2O$ single crystal and $K_3[Tc_2Cl_8]\cdot 2H_2O$ solution in hydrochloric acid are shown in Figs 5 and 6, respectively. The EPR spectra of polycrystalline specimens are, as a rule, structureless lines with half-width $\sim$ 500 Œ and effective *g*-factor $g_{eff} = 2.09\pm0.02$. Clearly defined fine structure is observed in the single-crystal spectra, though their parameters are similar to those listed above. Well-resolved spectra of solutions of these complexes can hardly be obtained because of the impossibility of achieving high technetium concentrations; where it is possible, the spectra are similar to that shown in Fig. 6.[4] EPR spectra of glassy frozen solutions of d^4-d^5 complexes have also been studied.[9, 52–54] It has been established that all dinuclear d^4-d^5 clusters studied have similar spectral patterns with the parameters coinciding within the limits of experimental error:

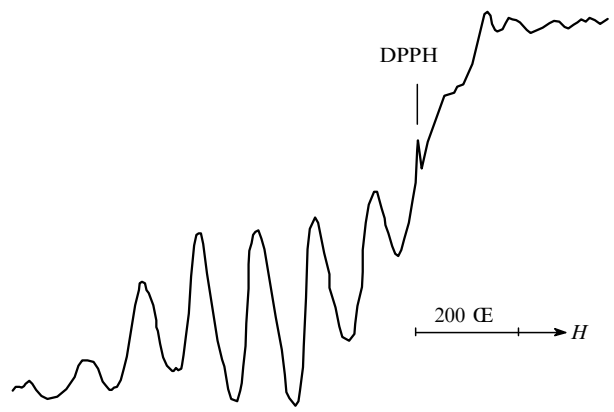


Figure 6. Typical EPR spectrum of Tc_2^{5+} complexes in solutions of HCl at 293 K $\{[Tc_2Cl_8]^{3-}$ in 4.0 M HCl$\}$.[4]

$g_{\|} = 1.85\pm0.03$, $g_{\perp} = 2.13\pm0.03$, $A_{\|} = -(188\pm5)\times10^{-4}$ cm^{-1}, $A_{\perp} = -(75\pm5)\times10^{-4}$ cm^{-1} and $P = (5\pm1)\times10^{-4}$ cm^{-1}. The spectra display strong anisotropy: lines of parallel orientation are observed in the region from 1600 to 5550 Œ, while those of perpendicular orientation and, probably, peaks of additional absorption are observed in the region from 2400 to 3900 Œ. From the data in Table 8 it can be seen that despite the chain structure of some of the compounds in question {e.g., $[Tc_2(AcO)_4]X$ (X = Cl, Br)}, intermolecular exchange interactions have no effect on their magnetic properties (the μ_{eff} values are close to the spin-only value corresponding to one unpaired electron and are temperature-independent).[2, 22–24, 51]

Thus, even qualitative analysis of the data on the magnetic susceptibility of d^4-d^5 complexes and their EPR spectra suggests that the only unpaired electron does occupy the $\delta^*(b_{1u})$ MO,[4] since only in this case can one expect that magnetic parameters will exhibit low sensitivity to the chemical nature of ligands. According to the results of SCF-X_α-SW calculations of the electronic structure of the $[Tc_2Cl_8]^{3-}$ ion,[9] the δ^* MO is the only MO of all unoccupied MOs to which the electrons of ligand atoms make no appreciable contribution (see Fig. 4). A more reliable proof of this fact is known that is independent of the results of theoretical calculations of the electronic structure.[3, 52, 53] Thus, the possible ground electronic states in the molecules of d^4-d^5 complexes and values of *g*-factors predicted by the theory of EPR spectra (the spin Hamiltonian method [55, 56]) have been considered. All possible 'reasonable' energy permutations of the MO levels were taken into account when analysing the experimental values of *g*-factors (see Fig. 4). From the data obtained it follows that qualitative agreement between theory and experiment can be achieved only if the b_{1u} MO is the highest occupied molecular orbital.

Dinuclear d^5-d^5 complexes are characterised by extremely short interatomic Tc—Tc distances ($\sim$ 2.04 Å), a chain structure, and idealised D_{4d} symmetry of the ligand environment (staggered conformation, see Fig. 1 *c*).[57, 58] The molecular and electronic structure of these compounds has been considered in detail.[2] According to calculations [2, 18] (see Fig. 4), the e_2 orbital formed by 'cross' overlap of the $4d_{xy}$ and $4d_{x^2-y^2}$ orbitals of two Tc atoms in the molecules of these compounds is the HOMO; formally, it is a low-energy δ bonding orbital. Considerable distortion of the idealised D_{4d} symmetry in the complexes results in the removal of degeneracy of the e_2 level and in partial increase in its δ bonding nature. Thus, the formation of formally quintuple M—M bonds in these compounds was first observed [57] in contrast to, *e.g.*, analogous d^5-d^5 osmium complexes with triple M—M bonds.[58, 59] Cotton *et al.*[58] interpreted the M—M bonds in d^5-d^5 technetium complexes as triple ones and their shortening as the result of changes in the diffuseness of the σ, π and δ components of these bonds due to changes in the formal technetium oxidation state.

From the data in Fig. 4 it follows that the $[Tc_2X_6]_n^{2n-}$ ions must be spin-paired (see Table 8). However, weak EPR signals of polycrystalline specimens of dinuclear d^5-d^5 technetium complexes are observed in some instances. The parameters of these signals indicate that the specimens contain small amounts (< 5%) of impurities (related paramagnetic d^4-d^5 complexes).

Polynuclear complexes (*clusters*). Most of these compounds have an island structure [51] (see Fig. 1 *d*, *e*, *f*), except for two octanuclear $[Tc_8Br_{13}]^{n-}$ clusters ($n = 0$, 1) with a chain structure.[60, 61] This would seemingly simplify the interpretation of the magnetic properties of this class of compounds, since in most cases there is no need to take into account intermolecular exchange interactions. However, the interpretation of the results of magnetochemical experiments on polynuclear technetium complexes appeared to be the most complex. This is first of all due to the complexity of the system of M—M bonds and high molecular weights of the compounds in question (and, hence, to the small contribution of spin-only paramagnetism to the magnetic susceptibility and to commensurable contributions of the Langevin diamagnetism and the Van Vleck paramagnetism), large relative

error of magnetic susceptibility measurements in the vicinity of zero values, strong effects of even small amounts of low-molecular-weight paramagnetic impurities as well as to a considerable uncertainty in the values of diamagnetic corrections for this class of compounds. In connection with the foregoing, the results of magnetochemical experiments were interpreted using EPR spectroscopy (as a tool for qualitative and semiquantitative analysis) and the results of theoretical calculations.

Trigonal-prismatic clusters. The following technetium compounds with this structure are known: $(Et_4N)_2.\{[Tc_6Br_6(\mu\text{-}Br)_6]Br_2\}$, $(Me_4N)_3\{[Tc_6X_6(\mu\text{-}X)_6]X_2\}$ (X = Cl, Br), $(Me_4N)_2[Tc_6Cl_6(\mu\text{-}Cl)_6]$, $(Bu^n_4N)_3\{[Tc_6Cl_6(\mu\text{-}Cl)_6]Cl_2\}$ and $(FeCp_2)_3\{[Tc_6Cl_6(\mu\text{-}Cl)_6]Cl_2\}$. The metal core of these clusters has the shape of a trigonal prism with an equilateral triangle as the base (see Fig. 1 *d*). The lateral edges of the prism correspond to the M – M bonds of formal order 3.0 – 4.0 (2.16 – 2.21 Å), while the edges of the prism base correspond to those of formal order 0.5 – 1.0 (2.55 – 2.75 Å). These clusters have the idealised D_{3h} symmetry.

Generally, there is no agreement between the calculated values[2, 54] and the experimental results (see Table 8). In fact, according to extended Hückel (EH) calculations, the $\{[Tc_6Br_6(\mu\text{-}Br)_6]Br_2\}^{2-}$ and $[Tc_6Cl_6(\mu\text{-}Cl)_6]^{2-}$ ions are in a spin-paired ground electronic state; however, experimental studies show that there is ~ 0.1 and ~ 0.2 unpaired electron per each cluster molecule, respectively, and that an EPR signal with $g_{eff} = 1.97$ is observed (Fig. 5 *d*, *e*) for a polycrystalline specimen of the latter compound. It should be noted that a weak temperature-dependent paramagnetic component of the total magnetic susceptibility of these clusters can hardly be associated with the presence of mechanical impurities of other paramagnetic polynuclear clusters, since according to X-ray phase analysis data obtained with an accuracy of 5% to 10% (sensitivity of the method), both compounds contain no impurities. Thus, this paramagnetic component can be due to either the nature of the compounds under consideration or the presence of a very small amount of paramagnetic mono- or di-nuclear technetium complexes. However, the fact that EPR signals with such parameters as those of the spectra shown in Fig. 5 *d*, *e* could not be observed for any of the paramagnetic impurities of mono- or di-nuclear technetium complexes possible in this case is against the latter assumption.

The interpretation of magnetochemical data for the compound with ferrocenium cations appeared to be all the more complex.[29] In fact, strong paramagnetism (~ 5 unpaired electrons per molecule) of this compound (see Table 8), the lack of similarity between its EPR spectrum (broad spectra with $g_{eff} \sim 2$) and spectra of compounds with similar anions and different tetraalkylammonium cations close in their size (Figs 7, 8; *cf.* Fig. 5), temperature-independent behaviour (down to ~ 4 K) of all magnetic parameters as well as physicochemical properties of other technetium and rhenium clusters with ferrocenium cations indicate altogether that their electronic structure is unusual and complex. In this connection, the magnetic properties of all compounds with ferrocenium cations will be considered in Section VI.

To a first approximation, the paramagnetism of $\{[Tc_6X_6(\mu\text{-}X)_6]X_2\}^{3-}$ ion corresponding to one unpaired electron per cluster (except for ferrocenium-containing compounds) is well described by theory[2, 34] (see Table 8, Fig. 4). However, no adequate description of EPR spectral parameters of these compounds ($g_{\parallel} \approx 2.00$, $g_{\perp} \approx 1.63$) can be obtained using the EH calculations. In fact, calculations of the electronic structure of trigonal-prismatic technetium clusters[34, 62, 63] suggest that the HOMO in these clusters can be either the a_2' (δ_{M-M}) MO or the a_2'' (π^*_{M-M}) MO. However, it has been reported[64] that none of these variants of the electronic structure as well as all other possible variants based on the energy permutations of the MOs in the HOMO – LUMO region can explain the values of *g*-factors observed experimentally (the analysis of *g*-factors was performed

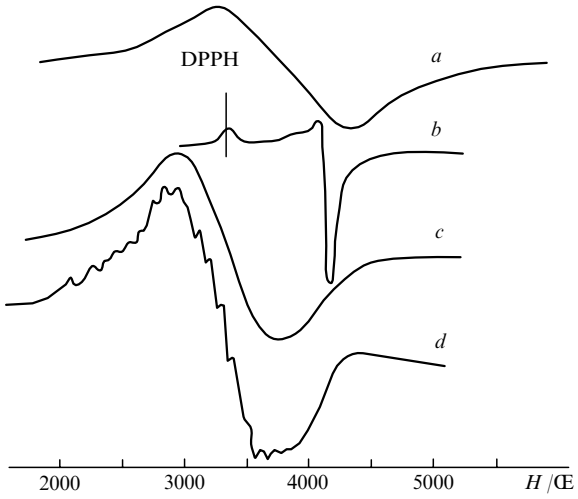


Figure 7. EPR spectra:[4, 18, 34] (*a*, *b*) $(Me_4N)_3\{[Tc_6(\mu\text{-}Br)_6Br_6]Br_2\}$ at 293 and 78 K, respectively; (*c*, *d*) $(Bu^n_4N)_2[Tc_6(\mu_3\text{-}Br)_5Br_6]$ at 293 and 78 K, respectively.

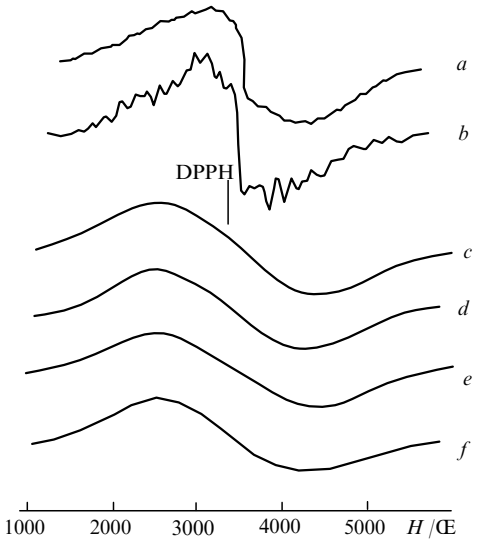


Figure 8. EPR spectra:[28, 29] (*a*, *b*) $(Bu^n_4N)_3\{[Tc_6(\mu\text{-}Cl)_6Cl_2]Cl_2\}$ at 300 and 78 K, respectively; (*c* – *e*) $(FeCp_2)_3\{[Tc_6(\mu\text{-}Cl)_6Cl_2]Cl_2\}$ at 300, 78 and 4 K, respectively; and (*f*) $(FeCp_2)_2[Re_2Br_8]$ at 300 and 78 K, respectively.

analogously to that for $d^4 - d^5$ complexes). Thus, magnetochemical experiments show that further refinement of theoretical MO schemes is required.

Such refinements have been carried out and reported.[18, 34, 64] According to the results obtained, the experimental magnetic and structural properties of trigonal-prismatic clusters are not contradictory to the idea that there is an MO with a_1' symmetry between the HOMO and the LUMO of these clusters. This orbital, composed mainly of diffuse 5*s* (5*p*) orbitals of the Tc atoms, is a $2\sigma_g$ bonding orbital in the direction of both vertical and horizontal M – M bonds in the metal core of the clusters (see Fig. 1 *d*). In other words, it seems likely that EH calculations[34, 62, 63] overestimate the interaction of δ* and π* MOs of the dimers in horizontal directions and underestimate the extent of participation of the 5*s* and $5p_z$ AOs in the formation of multiple M – M bonds.

In conclusion of this Section let us consider the interpretation of magnetic and other physicochemical properties of certain trigonal-prismatic technetium clusters. For instance, the analysis of the magnetic susceptibility of the cluster $(Me_4N)_2$.

.$[Tc_6(\mu\text{-}Cl)_6Cl_6]$ (see Table 8) shows that it obeys the Curie–Weiss law; a weak signal with a relative intensity of 0.2 of that of the $[Tc_6X_{14}]^{3-}$ signal and $g_{eff} \approx 1.97$ is observed in the EPR spectra of $[Tc_6(\mu\text{-}Cl)_6Cl_6]^{2-}$, which means that the compound under consideration is paramagnetic.[34] Since the $[Tc_6(\mu\text{-}Cl)_6Cl_6]^{2-}$ ion has an even number of 'metallic' electrons, paramagnetic properties can be manifested if the ground electron state is a triplet. Weak EPR signals and small μ_{eff} values as compared to those expected from the theory for the triplet state suggest that only a part of $[Tc_6(\mu\text{-}Cl)_6Cl_6]^{2-}$ clusters is paramagnetic in real crystals. Assuming that the relative intensity of the EPR signal (0.2) corresponds to the portion of triplet paramagnetic clusters, one can evaluate the magnetic moment of the hypothetical paramagnetic cluster using the formula $\mu^2 = \mu_{eff}^2/0.2$ (see Ref. 33); the result obtained ($\mu = 2.77\ \mu_B$) is rather close to the theoretical magnetic moment of a triplet species with $g_{eff} = 1.97$. Attempts to explain experimentally observed temperature dependences of the magnetic susceptibility and intensity of the EPR signal by the influence of the Boltzmann population of the triplet excited state, intermolecular exchange interactions or splitting of the triplet state levels in the crystal field have failed.

The simultaneous presence of singlet and triplet $[Tc_6(\mu\text{-}Cl)_6Cl_6]^{2-}$ clusters in crystals can be explained by sensitivity of the multiplicity of the ground state of the cluster to slight changes in its structure. In real crystals, a transition from the singlet ground state of the cluster to its triplet state can occur due to the presence of defects (vacancies, dislocations, disorder in the ligand environment, *etc*.) or, which is more probable in our opinion,[64] due to fast kinetic $S-T$ exchange with involvement of delocalised MOs formed mainly by the $5s$ ($5p$) orbitals of the Tc atoms.

The latter assumption is also supported by the long-wave IR spectra of trigonal-prismatic technetium clusters (Fig. 3) and unusual physicochemical properties of clusters with ferrocenium cations. In fact, the properties of the last-mentioned compounds taken altogether can be explained [28, 29] as a result of the formation of conduction bands and, perhaps, heavy-fermionic bands formed involving delocalised $5s$ ($5p$) orbitals of the Tc atoms and $4s$ orbitals of the Fe atoms of ferrocenium cations. The values of the g-factor in the EPR spectra of these compounds, close to that of the free electron, metallic type of the temperature dependence of conductivity, and unusual temperature dependence of the Mössbauer and X-ray photoelectron spectra are evidence for the formation of such bands. A more detailed theoretical interpretation of these properties will be given in Section VI of this review.

Tetragonal-prismatic clusters. This group comprises the following compounds: $\{[Tc_8(\mu\text{-}Br)_8Br_4]Br\}\cdot 2H_2O$, $[H(H_2O)_2]\cdot[Tc_8(\mu\text{-}Br)_8Br_4]Br\}$, $[H(H_2O)_2]_2\{[Tc_8(\mu\text{-}Br)_8Br_4]Br_2\}$, $(Bu^n_4N)_2\cdot\{[Tc_8(\mu\text{-}Br,I)_8(Br,I)_4]I_2\}$, $(FeCp_2)_2\{[Tc_8(\mu\text{-}Br)_8Br_4]Br_2\}$. Clusters belonging to this type are close in structure to the trigonal-prismatic ones. Their major distinction lies in the fact that in this case the metal core of the cluster is a prism with a rhombus in its base (Fig. 1*e*). According to the conventional count rule of valence electrons in clusters with acido ligands,[65, 66] the first of the above compounds must have 43, while each of the others must have 44 'metallic' electrons. The calculated electronic structure of a cluster with 44 valence electrons is shown in Fig. 4.[34, 62] As can be seen, these compounds must be spin-paired, whereas the $[Tc_8Br_{13}]\cdot 2H_2O$ cluster must possess a trivial paramagnetism with μ_{eff} corresponding to one unpaired electron. Indeed, the experimental data (see Table 8) show that only the compound $[Tc_8Br_{13}]\cdot 2H_2O$ has unpaired electrons; other clusters are characterised by TIP with large χ'_M values due to the high molecular weights of the clusters and their structural peculiarities [χ'_M (TIP) = $(570\pm150)\times 10^6$ CGSE units).

Magnetic properties of the ferrocenium-containing bromide octanuclear cluster are of particular interest. From the data in Table 8 it can be seen that paramagnetism of this compound obeys the Curie–Weiss law and corresponds to about two unpaired electrons per ferrocenium cation. No EPR signals of this compound are observed either at room temperature or at a liquid nitrogen temperature. Comparison of experimental results with the magnetic properties of ferrocenium-containing trigonal-prismatic chloride clusters considered above and $(FeCp_2)_2[Re_2Br_8]$ (this compound possesses trivial paramagnetism corresponding to about two unpaired electrons per formula unit and signals with $g_{eff} = 2.003$ are observed in its EPR spectra [28, 29]) shows that: (1) the EPR signals of all compounds in question are not due to localisation of the unpaired electrons on ferrocenium cations (this is also confirmed by the absence of EPR spectra of ferrocenium chloride and other ferrocenium compounds under the same conditions); (2) the EPR signals of the above clusters cannot also be due to localisation of the unpaired electrons on the cluster fragments, since in this case the recorded EPR spectra would be similar to those of the clusters with tetraalkylammonium cations; and (3) the paramagnetism of ferrocenium cations can affect the overall static magnetic susceptibility. Thus, it is most likely that all experimental facts as well as other unusual properties of the compounds under study,[28, 29] are due to fast dynamic electron transfer from the anion to the cation over distances 5 to 6 Å in a band formed by the overlap of upper ns (np) AOs of the cluster anions and ferrocenium cations (see also Section VI).

Octahedral clusters. This group comprises the following compounds: $(Bu_4N)_2[Tc_6(\mu_3\text{-}Br)_5Br_6]$, $[H_3O(H_2O)_3]_2\cdot[Tc_6(\mu_3\text{-}Br)_5Br_6]$ and $[H_3O(H_2O)_3]_2[Tc_6(\mu_3\text{-}Br)_5Br_6]\cdot 4H_2O$ (see Table 8), which are characterised by octahedral metal cores (see Fig. 1*f*). However, in contrast to the classical $[M_6X_8]^{4+}$ clusters (M = Mo, W; X = Cl, Br, I),[66] three of the eight positions of the bridging halide ligands in the technetium clusters remain statistically unoccupied. This effect of the distortion of octahedral clusters leads to their stabilisation despite the presence of nine 'excess' metallic electrons as compared to the stable electronic configuration of the $[M_6X_8]^{4+}$ clusters. The above technetium clusters each contain 33 valence electrons. Their electronic structures are depicted schematically in Fig. 4. It can be seen that these clusters possess trivial paramagnetism with μ_{eff} corresponding to one unpaired electron, which is confirmed by the data in Table 8. A typical EPR spectrum of one of the compounds in question shown in Fig. 7 is characterised by hyperfine structure and $g_{eff} \approx 2$.

Thus, the magnetochemical studies [18, 34] have shown that it is of crucial importance to know experimental magnetic properties of the maximum possible number of technetium compounds. Magnetochemistry of di- and polynuclear technetium clusters is of particular interest, since the magnetochemical studies of these compounds in combination with other methods of physicochemical analysis and theoretical calculations make it possible, first, to identify the above compounds and reveal the presence of impurities and, second, to study the electronic structure of these clusters that often have no close analogues. It should be noted that in some instances magnetochemical studies in combination with X-ray studies can provide valuable information on the composition and the formal oxidation state of technetium. For example, in such a way the formal charges of cluster anions in the compounds $\{[Tc_8Br_4(\mu\text{-}Br)]_8Br\}\cdot 2H_2O$, $[H(H_2O)_2]\{[Tc_8Br_4(\mu\text{-}Br)_8]Br\}$, $[H_3O(H_2O)_3]_2[Tc_6(\mu_3\text{-}Br)_5Br_6]$ and $[H_3O(H_2O)_3]_2[Tc_6(\mu_3\text{-}Br)_5Br_6]\cdot\cdot 4H_2O$ [9, 61, 67, 68] have been determined. In fact, it was impossible to locate hydrogen atoms in the structures of these clusters using the results of X-ray studies only; however, magnetic measurements made it possible to determine the number of unpaired electrons in the anions and, hence, the number of 'metallic' electrons, the oxidation state of technetium and thereby the anionic charges in the clusters.

IV. X-Ray photoelectron study of the structure of technetium complexes

1. Binding energies of the core electrons of technetium atoms

Table 9 presents the binding energies of the core electrons (E_b) in technetium clusters and some mononuclear complexes. It is noteworthy that the lines corresponding to E_b(Tc $3d_{5/2}$) are singlets in all compounds; judging by the half-widths of the lines ($l_{1/2} \leqslant 2.0$ eV), it is impossible to assign them to two or more chemically or structurally nonequivalent types of the Tc atoms. This conclusion is of particular importance for clusters with fractional oxidation state of technetium and $[Tc_2X_6]^{2-}$ anions

Table 9. Binding energies of the core electrons (E_b/eV) of Tc and halogen atoms in the X-ray photoelectron spectra of technetium compounds and the effective charges on Tc atoms calculated by the Pauling electronegativities (EN) and EH methods.[70–74]

Compound	Tc oxidation state	E_b(Tc3$d_{5/2}$)	$l_{1/2}$ /eV	E_b(Cl2$s_{1/2}$) [E_b(Br3$p_{3/2}$)] {E_b(I4$d_{5/2}$)}	Z_{EN} (Z'_{EN})	Z_{EH} (Z'_{EH})
$K[TcO_4]$ (**9**)	+7.0	259.0	1.8	–	1.60 (1.60)	3.854 (3.92)
$NH_4[TcO_4]$ (**10**)	+7.0	258.9	1.5	–	(1.57)	(3.85)
$(FeCp_2)[TcO_4]$ (**10′**)	+7.0	258.9	1.5	–	(1.57)	(3.85)
$Na[TcO_4]\cdot nH_2O$ (**11**)	+7.0	258.9	1.5	–	(1.57)	(3.85)
$Ni[TcO_4]_2\cdot nH_2O$ (**12**)	+7.0	259.1	1.5	–	(1.63)	(4.00)
$Co[TcO_4]_2\cdot nH_2O$ (**13**)	+7.0	259.2	1.7	–	(1.66)	(4.08)
$Ca[TcO_4]_2\cdot nH_2O$ (**14**)	+7.0	259.2	1.6	–	(1.66)	(4.08)
$Ba[TcO_4]_2\cdot nH_2O$ (**15**)	+7.0	259.0	1.8	–	(1.60)	(3.92)
$(Ph_4As)[TcO_4]$ (**16**)	+7.0	258.4	1.3	–	(1.41)	(3.46)
$(Bu^n_4N)[TcO_4]$ (**17**)	+7.0	258.7	1.7	–	(1.49)	(3.70)
Tc_2S_7 (**18**)	+7.0	254.7	1.4	–	0.31 (0.22)	(0.65)
$K_2[TcOCl_5]$ (**19**)	+5.0	257.6	1.6	269.0	1.00	–
$(Bu^n_4N)[TcOCl_4]$ (**20**)	+5.0	257.4	1.5	268.9	1.05	2.312 (2.40)
$(Bu^n_4N)[TcOBr_4]$ (**21**)	+5.0	256.5	1.6	[181.4]	0.85	(2.00)
$K_3[Tc_2Cl_8O_2]$ (**22**)	+4.5	256.8	1.4	268.9	1.08 (0.85)	–
Tc_2O_5 (**23**)	+5.0	256.6	1.8	–	1.72 (0.80)	–
$Tc_2O_5\cdot nH_2O$ (**24**)	+5.0	256.0	1.7	–	1.72 (0.65)	–
TcO_2 (**25**)	+4.0	255.2	1.8	–	1.52 (0.38)	(0.9)
$TcO_2\cdot nH_2O$ (**26**)	+4.0	255.4	2.0	–	1.52 (0.43)	(0.9)
$K_2[TcCl_6]$ (**27**)	+4.0	257.0	1.3	269.2	0.86	1.793 (1.793)
$(FeCp_2)_4[H_3O(H_2O)_4]_2[TcCl_6]_3$ (**27′**)	+4.0	257.0	1.5	269.1	0.86	1.793
$K_2[TcBr_6]$ (**28**)	+4.0	256.2	1.6	[181.4]	0.69	(1.60)
$(NH_4)_2[TcBr_6]$ (**29**)	+4.0	256.2	1.5	[181.4]	0.69	(1.60)
$[TcPy_2Cl_4]$ (**30**)	+4.0	256.8	1.6	268.8	0.83	–
$K_2[TcI_6]$ (**31**)	+4.0	255.6	1.6	{~48.0}	0.46	0.934 (1.20)
$(NH_4)_2[TcI_6]$ (**32**)	+4.0	255.5	1.5	{~48.0}	0.46	0.934 (1.20)
$(Bu^n_4N)_2[Tc_2Cl_8]$ (**33**)	+3.0	255.8	1.3	268.5	0.88 (0.54)	1.445 (1.445)
$[Tc_2(AcO)_4Cl]$ (**34**)	+2.5	255.8	1.8	268.3	0.91 (0.54)	1.206 (1.30)
$K[Tc_2(AcO)_4Cl_2]$ (**35**)	+2.5	255.8	1.6	268.2	0.92 (0.54)	–
$[Tc_2(AcO)_4Br]$ (**36**)	+2.5	255.7	1.6	[181.4]	0.87 (0.49)	–
$K_3[Tc_2Cl_8]\cdot nH_2O$ (**37**)	+2.5	255.5	1.8	269.0	0.80 (0.40)	1.065 (1.065)
$Tc_4O_5\cdot nH_2O$ (**38**)	+2.5	255.9	1.8	–	1.25 (0.58)	–
$K_2[Tc_2Cl_6]$ (**39**)	+2.0	254.9	1.6	268.9	0.73 (0.30)	0.704 (0.704)
$K_2[Tc_2Br_6]\cdot nH_2O$ (**40**)	+2.0	254.6	1.7	[181.4]	0.62 (0.20)	–
$(Et_4N)_2\{[Tc_6(\mu\text{-}Br)_6Br_6]Br_2\}$ (**41**)	+2.0	254.7	1.2	[181.1], [182.6]	0.60 (0.22)	(0.55)
$(Me_4N)_3\{[Tc_6(\mu\text{-}Br)_6Br_6]Br_2\}$ (**42**)	+1.83(3)	254.8	1.2	[181.1], [182.5]	0.60 (0.25)	(0.65)
$(Me_4N)_3\{[Tc_6(\mu\text{-}Cl)_6Cl_6]Cl_2\}$ (**43**)	+1.83(3)	255.0	1.3	268.8, 270.6	0.70 (0.32)	(0.76)
$(FeCp_2)_3\{[Tc_6(\mu\text{-}Cl)_6Cl_6]Cl_2\}$ (**43′**)	+1.83(3)	255.0	1.3	268.8, 270.6	0.70 (0.32)	(0.76)
$(Bu^n_4N)_3\{[Tc_6(\mu\text{-}Cl)_6Cl_6]Cl_2\}$ (**43″**)	+1.83(3)	255.0	(1.4)	268.8, 270.6	0.70 (0.32)	(0.76)
$(Me_4N)_2[Tc_6(\mu\text{-}Cl)_6Cl_6]$ (**44**)	+1.66(6)	255.3	(1.4)	268.9, 270.7	0.70 (0.42)	0.597 (0.597)
$\{[Tc_8(\mu\text{-}Br)_8Br_4]Br\}\cdot 2H_2O$ (**1**)	+1.625	254.7	(1.2)	[181.1], [182.6]	0.60 (0.22)	(0.55)
$[H(H_2O)_2]_2\{[Tc_8(\mu\text{-}Br)_8Br_4]Br_2\}$ (**3**)	+1.5	254.7	(1.4)	[181.0], [182.5]	0.55 (0.42)	(0.55)
$(FeCp_2)_2\{[Tc_8(\mu\text{-}Br)_8Br_4]Br_2\}$ (**3′**)	+1.5	255.2	(1.4)	[181.0], [182.5]	0.70 (0.42)	(0.60)
$[H_3O(H_2O)_3]_2[Tc_6(\mu_3\text{-}Br)_5Br_6]\cdot nH_2O$ (**6**)	+1.5	255.3	(1.8)	[181.1], [182.5]	0.55 (0.42)	(0.90)
$(Bu^n_4N)_2\{[Tc_8(\mu\text{-}X)_8X_4]I_2\}$ (**45**) (X = 0.5 Br + 0.5 I)	+1.5	254.6	(1.5)	[181.0], [182.5] {48.4}, {49.8}	0.52 (0.17)	–
$\{[Tc_8(\mu\text{-}I)_8I_4]I\}\cdot nH_2O$ (**46**)	+1.625	254.5	(1.3)	{48.4}, {49.8}	0.49 (0.17)	–
$(FeCp_2)_3\{[Tc_6(\mu\text{-}I)_6I_6]I_2\}$ (**46′**)	+1.5	254.4	(1.4)	{48.3}, {49.6}	0.49 (0.17)	–
TcC (**47**)	0	253.9	(1.5)	–	0 (0)	(0)
Tc (metal) (**48**)	0	253.9	(1.0)	–	0 (0)	0 (0)

Notes. The binding energies are given relative to a peak from adsorbed vapours of diffusion oil [E_b(C1s) = 284.3 eV]. The errors of the binding energy determination are ±0.2 eV, those of half-widths $l_{1/2}$ are ±0.1 eV. The binding energies of bridging atoms are underlined. The Z'_{EN} values were determined for compounds with M – M bonds, pertechnetates and binary compounds only from the correlation for mononuclear complexes (curve *a* in Fig. 9). The Z'_{EH} values were determined only for those compounds for which the experimental chemical shifts in X-ray emission spectra[75–77] and X-ray photoelectron spectra[70–74] are known.

(see Table 9) in which the Tc atoms formally either have different oxidation state or occupy strongly nonequivalent positions in the structure. Thus, equalisation of the electron density on technetium atoms occurs in all complexes. For most clusters such an equalisation of the electron density due to the formation of multiple M–M bonds could be assumed on the basis of their structural,[1,2,19,31,51,67] magnetic,[18,34] spectroscopic[8,52,53,54] and other physicochemical properties; however, in the case of $[Tc_2X_6]^{2-}$ compounds and octanuclear clusters a conclusion that the Tc atoms are structurally nonequivalent would be the most probable.[19,57,67,69] However, the half-widths of the Tc $3d_{5/2}$ lines in the X-ray photoelectron spectra of these compounds are even smaller as compared to half-widths of the same lines in the spectra of other technetium complexes including mononuclear ones.[70–74] This indicates strong delocalisation of the electron density in such clusters.

It is known that the chemical shifts in X-ray emission and X-ray photoelectron spectra often correlate with the effective charge on the atom considered.[75—78] The method based on Pauling electronegativities (EN)[78–80] is one of the simplest methods used in the effective charge calculations. As a rule, the effective charges (Z_{EN}) calculated using this method correlate almost linearly with binding energies.[78–80] However, the EN method makes it possible to calculate the Z_{EN} values determined only by conventional valence bonds. If an additional bonding occurs in a compound (*e.g.*, due to hydrogen or π-donor bonds, trans-effect, dative bonds, multiple homopolar bonds, surface effects, *etc.*), then the Z_{EN} values can differ substantially from the experimental effective charges; however, this difference itself will be indicative of such additional effects.[79,80] It should be noted[79,80] that effective charges determined experimentally by different physicochemical or theoretical methods can differ considerably for the same compound, since each method is characterised by specific 'sensitivity' to an effective space region around the atom in question.

Using the EN calculations carried out in the framework of a unified approach,[70,74] it has been possible to reveal the reasons for changes in the binding energies of the core electrons of the Tc atoms; this is necessary for determining the oxidation state of technetium in newly synthesised compounds. In other words, this method allows one to understand specific features of the structure of technetium compounds with M–M bonds. It should be noted that, although EN calculations are approximate and arbitrary, this method has some advantages over the traditionally used purely qualitative description of changes in the binding energies of the core electrons depending on the oxidation state of the atom and on the electronegativity of the ligands surrounding this atom, since it relates these two parameters on which the binding energy depends in most instances. Of course, this method lacks sufficient physical grounds characteristic of more rigorous computational methods such as, *e.g.*, the MO LCAO method. However, as a rule, EN calculations make it possible to obtain almost linear correlations between the effective charges[78–80] and the binding energies, especially, for compounds of similar composition and structure.

The Z_{EN} values were calculated using the following electronegativities (χ) of technetium obtained by interpolating the χ values for Re, Mo, Mn, and Cr in different oxidation states:[79,80] $\chi(Tc^{I}) = 1.10$, $\chi(Tc^{II}) = 1.40$, $\chi(Tc^{III}) = 1.60$, $\chi(Tc^{IV}) = 1.80$, $\chi(Tc^{V}) = 1.95$, $\chi(Tc^{VI}) = 2.10$ and $\chi(Tc^{VII}) = 2.25$. The Z_{EN} calculations were performed[70–74] according to the Batsanov procedure[79,80] assuming the absence of M–M bonds and other peculiarities of the molecular, crystal and electronic structure capable of affecting the χ(Tc) value. Thus, it has been assumed *a priori* that in the case of systematic deviations of Z_{EN} values from the experimental effective charges (Z'_{EN}) for the clusters (see Table 9) these deviations must be due to a specific effect of the M–M bonds, since the nature of the M–X bonds in mono-, di- and poly-nuclear clusters remains unchanged in most instances, except for the M–μ-X and M–X_{ax} bonds.

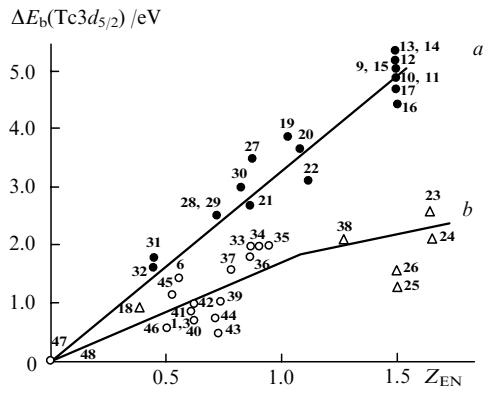


Figure 9. Dependence of the chemical shifts of binding energies of the core electrons [ΔE_b(Tc $3d_{5/2}$)] in technetium compounds on the effective charge on the Tc atoms (Z_{EN}) calculated by the Pauling electronegativities method (the numbering of points corresponds to that of the compounds in Table 9): (*a*) correlation for mononuclear complexes (filled circles); (*b*) correlation for compounds with M–M bonds, di- and polynuclear clusters with acido ligands (open circles) and for binary compounds (sulfides and oxides, open triangles).[72] For visual aids, correlation lines are drawn.

The dependence of the ΔE_b(Tc $3d_{5/2}$) values on Z_{EN} for technetium complexes is shown in Fig. 9. It can be seen that all experimental points fall on two curves. The curve *a* closely resembles an almost straight line and describes the dependence ΔE_b(Tc $3d_{5/2}$) = $\varphi(Z_{EN})$ for compounds containing no Tc–Tc bonds. The points that obey the dependence ΔE_b(Tc $3d_{5/2}$) = $\varphi'(Z'_{EN})$ and correspond to the technetium compounds with strong Tc–Tc bonds and to binary compounds fall on curve *b*. The curve *b* in Fig. 9 is much below the curve *a*. This is a direct consequence of neglecting the effect of homopolar multiple Tc–Tc bonds on the electronegativity of Tc atoms, which leads to overestimation of the Z_{EN} values as compared to the 'true' effective charges (Z'_{EN}) obtained within the framework of the EN model. Thus, the Z'_{EN} values for technetium clusters can be determined either by introducing some corrections to the technetium electronegativity or from experimental ΔE_b(Tc $3d_{5/2}$) values using the correlation curve for mononuclear complexes (see Fig. 9, curve *a*).

Comparison of the curves *a* and *b* in Fig. 9 as well as comparison of Z_{EN} and Z'_{EN} values (see Table 9) shows that the formation of the metal–metal bonds in technetium clusters leads to a decrease in Z_{eff} on the metal atoms. It should be noted that no analogous decrease in Z_{eff} is observed upon the formation of M–M bonds in clusters of other transition *d* elements with similar structures and properties. At first glance, it may appear that this technetium 'anomaly' is only a consequence of inadequacy of the procedure for calculating the Z_{EN} values. However, this is not the case. To make sure that Z_{eff} values decrease as the M–M bonds are formed in the case of technetium, it is sufficient to compare the experimental values of changes in the binding energies of the core electrons (ΔE_b) for some transition *d* elements (Table 10); for molybdenum, the opposite is observed (Z_{eff} increase as the M–M bonds are formed), while the Z_{eff} values remain unchanged for rhenium and most of other elements. In fact, from the data in Table 10 and Refs 19, 51, 70–74, 78 and 81–85 it follows that the mean change in the ΔE_b value corresponing to a change of unity in the formal oxidation state of a metal M (M = Tc, Re, and Mo) in complexes with similar stoichiometry and structures is ~ 0.7 eV. Analogous changes in ΔE_b on going from mononuclear d^3 complexes to dinuclear d^4–d^4 ones are +1.2 eV for Tc, +0.7 eV for Re and −3.3 eV for Mo. Data obtained by X-ray emission spectroscopy[86–88] allowed one to draw analogous conclusions that Z_{eff} values increase in the case of the Mo–Mo bonds.

Table 10. Chemical shifts of binding energies (ΔE_b) of the core electrons of transition metals in their clusters relative to those of pure metals (averaged values, according to the reported data [19, 51, 70–74, 78, 81–85]).

Cluster	ΔE_b / eV	Cluster	ΔE_b / eV
$[Re_2Cl_8]^{2-}$	3.0	$[Ta_6Cl_{12}]^{2+}$	2.6
$(ReCl_3)_n$	2.7	$[Ta_6Cl_{12}]^{4+}$	2.6
$(ReCl_2)_n$	2.0	$[Mo_2Cl_8]^{4-}$	3.6
$[Nb_6Cl_{12}]^{2+}$	2.6	$(MoCl_2)_n$	3.3
$[Nb_6Cl_{14}]^{2+}$	2.6	$[Rh_2(AcO)_4]$	2.4
$[Tc_6(\mu\text{-}Cl)_6Cl_6]^{n-}$	1.0	$[L_2Pd(AcO)_2]_2$	2.7
$[Tc_2Cl_8]^{2-}$	1.9	$[Cr_2Cl_9]^{3-}$	2.6
$[Tc_2Cl_6]^{2-}$	1.1		

It is clear that in the general case the effective atomic charge must depend on the formal order of the bond between this atom and another atom, since a redistribution of the electron density of valence electrons mostly occurs as the bond order increases. This appreciably changes the conditions of shielding of the positive nuclear charge by outer electrons. Simultaneously, when two atoms approach each other as a result of the increase in the order of the interatomic bond, their inner atomic electron shells must undergo an increasing repulsion, which brings about the opposite result, *viz*., a decrease in the extent of shielding of the positive nuclear charge due to the formation of the multiple bond. Since each physical method is characterised by specific 'sensitivity' to an effective space region around the atom M, the net change in Z_{eff} will strongly depend on many factors and can be either positive or negative, or be equal to zero.

A theoretical explanation for the effect of a decrease in Z_{eff} on the Tc atoms in the formation of M–M bonds consists in the following:[64] in contrast to clusters of other *d* elements, it is highly probable that the outer 5*s* (5*p*) AOs of technetium clusters participate in the formation of 'metallic' bonding MOs. Thus, it has been shown experimentally [64] and theoretically [89] that the a_1' MO composed mainly of 5*s* (5*p*) orbitals of six Tc atoms represents the HOMO in the trigonal-prismatic technetium clusters $[Tc_6X_{14}]^{3-}$ (X = Cl and Br) (see also Section III). Since these outer AOs possess an increased capability of shielding the positive nuclear charge, their participation in the formation of the M–M bonds results in a decrease in Z_{eff}. It should be noted that an analogous conclusion that Z_{eff} values of the Tc atoms are decreased upon the formation of M–M bonds was drawn on the basis of analysis of changes in the chemical shifts in the $K_{\alpha 1}$ X-ray emission spectra of technetium compounds.[76, 77]

The effective charge on the Tc atoms have also been evaluated using extended Hückel calculations.[71–73] This semiempirical MO method allows one to take into account the effect of M–M bonds. Therefore, the effective charge obtained by EH calculations (Z_{EH}) can correlate directly with the chemical shifts in the spectra of Tc compounds without introduction of corrections for the M–M bonds. However, a strong parametrisation effect on the results of calculations hampers the use of EH calculations. To diminish this effect, only the results of calculations for the chloride technetium complexes ($[TcCl_6]^{2-}$, $[Tc_2Cl_8]^{2-}$, $[Tc_2Cl_8]^{3-}$, $[Tc_2Cl_6]^{2-}$, and $[Tc_6Cl_{14}]^{3-}$) were used. The more detailed consideration of the general procedure for calculations and parametrisation, and the procedure for determination of the effective charge (Z'_{EH}) using EH calculations and the data of X-ray emission spectroscopy (XES) and X-ray photoelectron spectroscopy (XPES) simultaneously is given in Section V. These values are listed in Table 9.

The dependence of ΔE_b(Tc $3d_{5/2}$) on Z_{EH} is shown in Fig. 10. Comparison of the data in Figs. 9 and 10 and the Z'_{EN} and Z'_{EH} values shows that Z_{eff} calculated by the EN and EH methods differ considerably; however, they are related by an unambiguous monotonic dependence. In addition, common to both mononuclear complexes and clusters is the observed dependence of the ΔE_b(Tc $3d_{5/2}$) values on Z_{EH} rather than on Z_{EN}. This is understandable since the EH calculations (in contrast to the EN calculations) take into account electronic effects due to the formation of the M–M bonds.

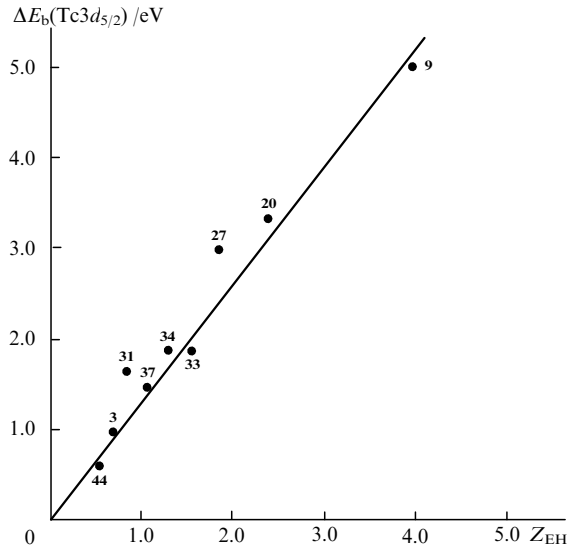


Figure 10. Dependence of the chemical shifts of binding energies of the core electrons ΔE_b(Tc $3d_{5/2}$) in technetium compounds on the effective charge on the Tc atoms (Z_{EH}) calculated by the EH method (the numbering of points corresponds to that of the compounds in Table 9).[72]

2. Binding energies of the core electrons of halogen atoms

Table 11 lists the binding energies of the core electrons of the halogen atoms [E_b(X)] in clusters of transition *d* elements. As can be seen, the E_b(X) values vary depending on the nature of the halogen–metal bonds. For technetium clusters, the smallest E_b(X) values have been found for axial halogen atoms in carboxylate dinuclear complexes with the 'lantern'-type structure (see Table 9). Since the $E_b(X_{ax})$ values are close to analogous values for pure ionic compounds,[78] it can be assumed that all Tc–X_{ax} bonds are ionic. It should also be noted that these types of bonds of halogen atoms are much weaker due to the trans-effect of multiple metal–metal bonds. Previously,[78, 84, 85] an analogous phenomenon has been observed experimentally for dinuclear Re and Rh complexes.

Table 11. Binding energies (E_b / eV)[a] of the core electrons of halogen atoms in clusters of transition *d* elements (averaged values, according to the reported data [19, 51, 70–72, 78, 81–85]).

Cluster-forming metal	E_b(Cl3$p_{3/2}$)			E_b(Br3$d_{5/2}$)			E_b(I4$d_{5/2}$)		
	ax	eq	bridge	ax	eq	bridge	ax	eq	bridge
Tc	197.2	198.0	199.5	67.7	67.7	69.2	–	48.4	49.8
Re	197.5	198.5	199.7	68.1	68.8	68.8	48.5	49.2	–
Mo	197.3	197.8	199.8	–	67.7	68.8	–	48.5	49.7
Rh	197.4	198.1	–	68.2	68.7	–	–	–	–
Pt	197.5	198.2	–	68.2	68.9	–	48.6	–	–
Nb	–	197.0	198.7	–	67.4	–	–	–	–
Ta	–	197.0	199.1	–	68.0	–	–	–	–
K[b]	197.5	–	–	67.8	–	–	–	–	–

Note. The following notations are used: ax is axial, eq is terminal (equatorial), and br is bridging. [a] The error of binding energy determination is ±0.4 eV. [b] Potassium halides. The binding energies are given relative to the C1*s* line (284.3 eV).

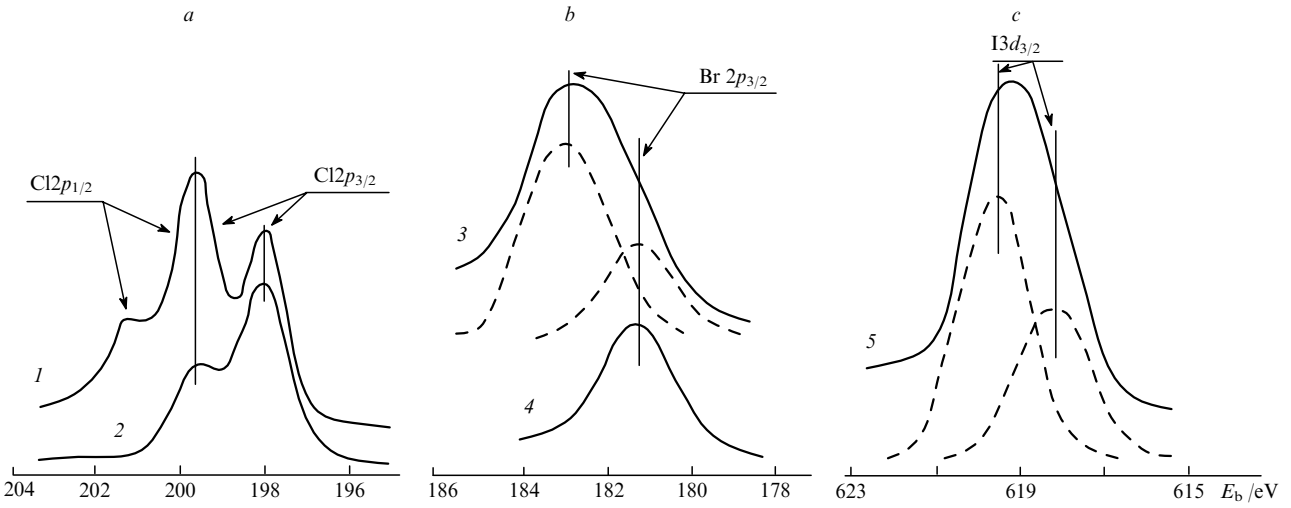


Figure 11. Binding energy X-ray photoelectron spectra of the core electrons of the halogen atoms in polynuclear (*1*, *3*, *5*) and mononuclear (*2*, *4*) chloride (*a*), bromide (*b*) and iodide (*c*) complexes: (*1*) $(Me_4N)_2[Tc_6Cl_{12}]$; (*2*) $K_2[TcOCl_5]$; (*3*) $[Tc_8Br_{13}]\cdot 2H_2O$; (*4*) $(NH_4)_2[TcBr_6]$; and (*5*) $[Tc_8I_{13}]\cdot 2H_2O$. Dashed lines represent the deconvolution of experimental spectra by the least squares method assuming a Lorentzian shape of single peaks.

The $E_b(X)$ values for the equatorial (terminal) halogen atoms in the technetium clusters correspond to the binding energies of the core electrons of the terminal halogen atoms in mononuclear halide complexes (see Table 9). The $Tc-X_{eq}$ bond lengths are also close to those of the Tc—X bonds in halide Tc^{V} and Tc^{IV} complexes.[1, 2, 31, 90, 91] The $E_b(X)$ values for these types of halogens indicate weak ionicity of the $Tc-X_{eq}$ bonds.[78]

The largest $E_b(X)$ values are observed for the bridging halogen atoms in polynuclear clusters (see Table 9); they are close to the $E_b(X)$ for the halogen elements,[78] which indicates that the Tc—(μ-X) bonds are covalent.

As can be seen from the data presented, the structure and composition of technetium complexes can be qualitatively and semiquantitatively judged from the $E_b(X)$ values of the halogen atoms. Indeed, the structures of polynuclear technetium clusters contain all three types of halogen atoms, whereas two lines corresponding to $E_b(X)$ of the terminal and bridging halogen atoms with relative intensities proportional to the stoichiometric amount of these halogen atoms in the cluster are observed in the X-ray photoelectron spectra of these compounds (Fig. 11). It is likely that the peaks corresponding to axial halogen atoms or halide ions are not observed in the spectra due to their low relative intensity.

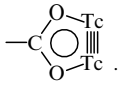
The 'sensitivity' of the chemical shifts in the X-ray photoelectron spectra to the coordination type of halide ligands can serve as a convenient tool for tentative analysis of the structure. In some instances, the data obtained by X-ray photoelectron spectroscopy significantly complement the information obtained by X-ray analysis and chemical analysis. Thus, an attempt to establish unambiguously the exact stoichiometric composition of a bromide–iodide octanuclear technetium cluster using X-ray analysis[92] and chemical analysis has failed. Only additionally taking the X-ray photoelectron spectra has made it possible to establish the stoichiometry, composition and structure of the cluster $(Bu^n_4N)_2[Tc_8(\mu\text{-}Br)_4(\mu\text{-}I)_4Br_2I_2]I_2$ (see Table 9).

3. Binding energy X-ray photoelectron spectra

The binding energy X-ray photoelectron spectra of a number of technetium compounds have been considered.[71–73] The experimental spectra have been compared with the results of theoretical SCF-X_α-SW calculations for K_2TcCl_6 [93] and $K_3Tc_2Cl_8\cdot 2H_2O$.[9] It has been shown that at a qualitative level the calculations represent satisfactorily the fine structure of X-ray photoelectron spectra in most cases. However, the spectra of solids are not always well resolved due to line broadening. The approximate character of the theoretical calculations makes it possible, as a rule, to determine only the order in which the MOs are arranged on the energy scale rather than the exact absolute values of their vertical ionisation potentials. Despite these drawbacks the following qualitative conclusions were drawn:[71–73]

1. The high-lying MOs (δ_{M-M} and δ^*_{M-M} orbitals according to the calculations and EPR spectroscopy data [9, 52, 53, 94]) appear to be separated in energy from other MOs on going from $[TcCl_6]^{2-}$ to $[Tc_2Cl_8]^{3-}$.

2. Replacement of Cl atoms by μ-bridging acetate ions results in a higher degree of mixing in energy between the π-components of the M—M and M—L bonds; however, the δ_{M-M} and δ^*_{M-M} components remain (though to a lesser extent) separated from other MOs. This is probably due to the formation of cyclic closed π-systems of the type



3. Replacement of the axial ligands in the $\{[Tc_2(AcO)_4]Cl_n\}^{(n-1)-}$ ($n = 1$ or 2) anion by Br^- does not result in considerable changes in the patterns of the binding energy spectra, which indicates a small contribution of AOs of the axial ligands to the δ_{M-M}, π_{M-M} and π_{M-L} MOs, since the axial ligands form mainly ionic bonds with the Tc atoms and only due to the trans-effect [78, 84, 85] do they somewhat weaken the σ component of the M—M bonds, which is hardly observed in this spectral region.

4. There is even greater separation in energy of the δ component of the M—M bond from other types of MOs in the complex $K_2[Tc_2Cl_6]$, which is due to specific features of the bond formation in d^5-d^5 complexes with an idealised D_{4d} symmetry. According to the data reported in Ref. 57, the formation of δ bonds in $K_2[Tc_2Cl_6]$ occurs due to 'cross' overlap of the $4d_{xy}$ and $4d_{x^2-y^2}$ orbitals of the Tc atoms. This results in considerable decrease in the vertical ionisation potential of δ MO, since the $4d_{x^2-y^2}$ AOs of technetium participate mainly in the formation of the σ bonds with ligands. It should be noted that this energy separation of the σ MO is not observed in the complex $K_2[Tc_2Br_6]$,[18] since the Br^- ions, being ligands of weaker field and lower electronegativity as compared to the Cl^- ions, do not cause such a substantial decrease in the vertical ionisation potential of δ MOs.

5. The formation of high-lying MOs in polynuclear clusters occurs mainly involving δ MOs and π MOs of dinuclear clusters,[2, 51, 62, 63, 64] which results in an increase in their vertical

ionisation potentials. Therefore, in most cases no low-energy lines corresponding to separated high-lying MOs are observed in the X-ray photoelectron spectra of polynuclear clusters and lines corresponding to all components of the M – M bonds are strongly mixed in energy. The exception is the complex $(Me_4N)_2[Tc_6Cl_{12}]$ and clusters with ferrocenium cations (peaks near the Fermi level are observed in their X-ray photoelectron spectra).[29] This is probably due to the formation of a conduction band in these compounds involving high-lying 5*s* (5*p*) orbitals of the Tc atoms.

V. Chemical shifts in X-ray K_α emission spectra of technetium compounds

In the preceding Section we have considered the X-ray photoelectron spectra of technetium compounds[70–74] and demonstrated their efficiency for studying the electronic structure of clusters. Here, the results of joint XES and XPES studies of the electronic structure of technetium compounds are presented and the experimental results obtained are compared with those of semiempirical EH calculations.

Table 12 presents the experimental and theoretical results.[75–77] The interdependence of the experimental chemical

Table 12. Experimental values of the chemical shifts in the X-ray emission spectra ($\delta E_{K_{\alpha 1}}$) and X-ray photoelectron spectra ($\Delta E_{3d_{5/2}}$) spectra of technetium compounds (with respect to metallic Tc) and the calculated effective partial charges on Tc atoms.[77]

Compound	Tc oxidation state	$\delta E_{K_{\alpha 1}}$ / meV	$\Delta E_{3d_{5/2}}$ / eV	Z_{EH}	Q_{5s}	Q_{5p}	Q_{4d}	q_{s+d}	q_s	q_d
$(FeCp_2)[TcO_4]$ (**10′**)	7.0	−233(8)	5.0(2)	3.85	1.00	−0.1	2.90	1.73(5)	0.28	1.45
$K[TcO_4]$ (**9**)	7.0	−234(4)	5.1(2)	3.854 [a]	0.779 [a]	−0.219 [a]	3.294 [a]	1.73(3)	0.28	1.45
				3.92	1.0	−0.1	3.0			
$(Ph_4As)[TcO_4]$ (**16**)	7.0	−227(8)	4.5(2)	3.46	0.9	0	2.55	1.69(5)	0.26	1.43
$Na[TcO_4]\cdot nH_2O$ (**11**)	7.0	−218(3)	–	3.85	–	–	–	1.63(2)	0.28	1.35
$(Bu^n_4N)[TcO_4]$ (**17**)	7.0	−198(4)	4.8(2)	3.70	0.97	−0.1	2.78	1.51(2)	0.27	1.24
Tc_2S_7 (**18**)	7.0	−72(50)	0.8(2)	0.65	0.45	−0.2	0.40	0.7(4)	0.19	0.51
$(Bu^n_4N)[TcOCl_4]$ (**20**)	5.0	−91(20)	3.5(2)	2.312 [a]	0.734 [a]	−0.237 [a]	1.815 [a]	0.82(13)	0.19	0.63
				2.40	0.81	−0.25	1.84			
$(Bu^n_4N)[TcOBr_4]$ (**21**)	5.0	−47(7)	2.6(2)	2.0	0.71	−0.2	1.29	0.54(5)	0.19	0.35
$[TcO_2Py_4Cl]\cdot 2H_2O$ (**49**)	5.0	−154(3)	–	–	–	–	–	1.23(2)	0.24	0.99
Tc_2O_5 (**23**)	5.0	−104(5)	–	–	–	–	–	0.91(3)	0.20	0.71
TcO_2 (**25**)	4.0	−89(2)	1.3(2)	0.90	0.5	−0.25	0.65	0.81(2)	0.19	0.62
TcS_2 (**50**)	4.0	−40(3)	–	–	–	–	–	0.50(2)	0.18	0.32
$K_2[TcF_6]$ (**51**)	4.0	−133(30)	–	2.6	–	–	–	1.09(19)	0.22	0.87
$K_2[TcCl_6]$ (**27**) [b]	4.0	−51(6)	3.1(2)	1.793 [a]	0.723 [a]	−0.283 [a]	1.353 [a]	0.57(4)	0.19	0.38
$(Me_4N)_2[TcCl_6]$ (**52**)	4.0	−36(5)	–	1.45	–	–	–	0.47(3)	0.18	0.29
$(Et_4N)_2[TcCl_6]$ (**53**)	4.0	−39(3)	–	1.50	–	–	–	0.49(2)	0.18	0.31
$(Bu^n_4N)_2[TcCl_6]$ (**54**)	4.0	−36(5)	–	1.45	–	–	–	0.47(3)	0.18	0.29
$K_2[TcBr_6]$ (**28**)	4.0	−14(5)	2.3(2)	1.60	0.84	−0.2	0.96	0.33(3)	0.18	0.15
$(NH_4)_2[TcBr_6]$ (**29**)	4.0	6(10)	–	–	–	–	–	0.20(3)	0.18	0.02
$(Me_4N)_2[TcBr_6]$ (**55**)	4.0	21(4)	–	–	–	–	–	0.11(3)	0.18	−0.07
$K_2[TcI_6]$ (**31**)	4.0	23(4)	1.7(2)	0.934 [a]	0.560 [a]	−0.450 [a]	0.824 [a]	0.09(9)	0.18	−0.09
				1.2	0.67	−0.2	0.73			
$(Et_4N)_2[TcI_6]$ (**56**)	4.0	24(6)	–	–	–	–	–	0.08(6)	0.18	−0.10
$(Bu^n_4N)_2[Tc_2Cl_8]$ (**57**) [b]	3.0	−52(5)	1.9(2)	1.445 [a]	0.648 [a]	−0.235 [a]	1.032 [a]	0.57(4)	0.19	0.38
$(Bu^n_4N)_2[Tc_2Br_8]$ (**58**)	3.0	−48(10)	–	–	–	–	–	0.55(7)	0.18	0.33
$K_2[Tc_2(SO_4)_4]\cdot 2H_2O$ (**59**)	3.0	−42(3)	–	–	–	–	–	0.51(2)	0.18	0.33
$[Tc_2(AcO)_4Cl_2]$ (**60**)	3.0	−42(6)	–	–	–	–	–	0.51(4)	0.18	0.33
$[Tc_2(AcO)_4Cl]$ (**34**)	2.5	−17(4)	1.9(2)	1.206 [a]	0.657 [a]	−0.222 [a]	0.771 [a]	0.35(3)	0.18	0.17
				1.30	0.65	−0.25	0.90			
$K_3[Tc_2Cl_8]\cdot nH_2O$ (**37**) [b]	2.5	19(8)	1.6(2)	1.065 [a]	0.647 [a]	−0.233 [a]	0.651 [a]	0.12(5)	0.18	−0.06
$Py_3[Tc_2Cl_8]$ (**61**)	2.5	34(10)	–	0.80	–	–	–	0.02(7)	0.18	−0.16
Tc_4O_5 (**38′**)	2.5	−16(16)	2.0(2)	1.40	0.66	−0.2	0.94	0.34(10)	0.18	0.16
$K_2[Tc_2Cl_6]$ (**39**) [b]	2.0	60(3)	1.0(2)	0.704 [a]	0.647 [a]	−0.209 [a]	0.266 [a]	−0.14(2)	0.20	−0.34
$(Et_4N)_2\{[Tc_6(\mu\text{-}Br)_6Br_6]Br_2\}$ (**41**)	2.0	40(4)	0.8(2)	0.55	0.62	−0.31	0.24	−0.02(2)	0.18	−0.20
$(Me_4N)_3\{[Tc_6(\mu\text{-}Br)_6Br_6]Br_2\}$ (**42**)	1.83(3)	42(4)	0.9(2)	0.65	0.63	−0.27	0.29	−0.03(2)	0.18	−0.21
$(Me_4N)_3\{[Tc_6(\mu\text{-}Cl)_6Cl_6]Cl_2\}$ (**43**)	1.83(3)	42(3)	0.5(2)	0.35	0.61	−0.40	0.14	−0.03(2)	0.18	−0.21
$(Me_4N)_2[Tc_6(\mu\text{-}Cl)_6Cl_6]$ (**44**) [b]	1.66(6)	0(8)	0.07(2)	0.597 [a]	0.555 [a]	−0.229 [a]	0.271 [a]	0.24(5)	0.18	0.06
$\{[Tc_8(\mu\text{-}Br)_8Br_4]Br\}\cdot 2H_2O$ (**1**)	1.625	49(3)	0.8(2)	0.55	0.63	−0.3	0.22	−0.07(5)	0.19	−0.26
$[H(H_2O)_2]_2\{[Tc_8(\mu\text{-}Br)_8Br_4]Br_2\}$ (**3**)	1.5	43(6)	0.8(2)	0.55	0.62	−0.3	0.23	−0.04(2)	0.18	−0.22
$[H_3O(H_2O)_3]_2[Tc_6(\mu_3\text{-}Br)_5Br_6]$ (**5′**)	1.5	0(2)	1.4(2)	1.0	0.61	0.20	0.59	0.24(1)	0.18	0.06
$[H_3O(H_2O)_3]_2[Tc_6(\mu_3\text{-}Br)_5Br_6]\cdot nH_2O$ (**6**)	1.5	42(6)	–	–	–	–	–	−0.03(2)	0.18	−0.21
$Tc(CO)_5Cl$ (**62**)	1.0	−46(12)	–	–	–	–	–	0.54(7)	0.18	0.36
$Tc(CO)_5Br$ (**63**)	1.0	−50(12)	–	–	–	–	–	0.56(7)	0.18	0.38
TcC (**47**)	0	−14(5)	0.02(2)	0	0.18	0	0.18	0.33	0.18	0.15

[a] Results of EH calculations. [b] These compounds were used to calculate C_{nl} and δ_{nl} in Eqn (1). The partial charges Q_{nl} and q_l were determined from Eqns (1) and (2) using the Z_{EH} effective charges and the Hartree – Fock approximation, respectively (see text).

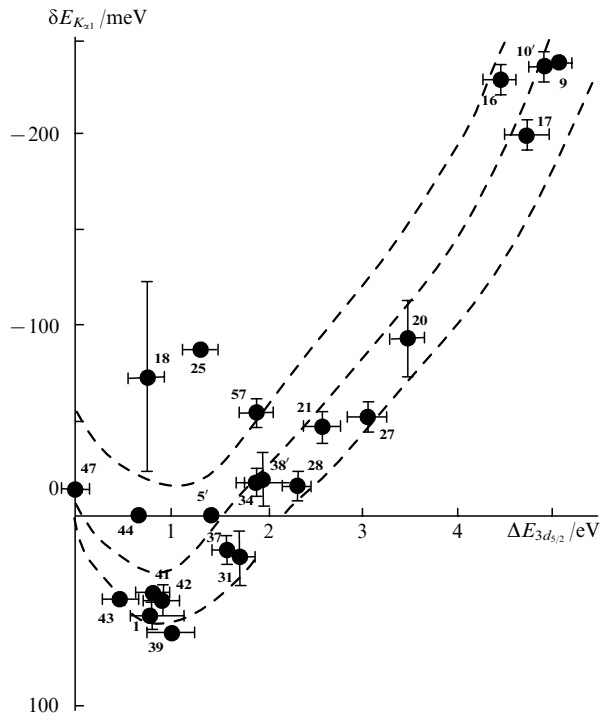


Figure 12. Correlation between the chemical shifts in the $K_{\alpha 1}$ X-ray emission spectra ($\delta E_{K_{\alpha 1}}$) and X-ray photoelectron spectra ($\Delta E_{3d_{5/2}}$) of technetium compounds[77] (the numbering of points corresponds to that of compounds in Table 12). The scatter of experimental data is shown by dashed lines.

shifts in the X-ray emission (δE) and X-ray photoelectron (ΔE) spectra is shown in Fig. 12.

According to the effective ion model,[98] the δE and ΔE values depend on the effective charge of the central atom (Q) as follows:

$$\delta E = C_{5s}Q_{5s} + C_{4d}Q_{4d} + Q_{5s}(Q_{5s} - 1)\delta_{5s} + Q_{4d}(Q_{4d} - 1)\delta_{4d} + Q_{5s}Q_{4d}\delta_{5s,4d}; \quad (1)$$

$$\Delta E = Q_{5s}\Delta E_{5s} + Q_{4d}\Delta E_{4d} + Q_{5s}(Q_{5s} - 1)\Delta_{5s} + Q_{4d}(Q_{4d} - 1)\Delta_{4d} + Q_{5s}Q_{4d}\Delta_{5s,4d} + \varphi_M, \quad (2)$$

where Q_{nl} is the partial charge remaining on an atom after the nl-electron has been involved in the formation of a bond, $C_{nl}(\Delta E_{nl})$ is the line shift in the X-ray emission spectrum (or in the X-ray photoelectron spectrum) after abstraction of the nl-electron; δ and Δ are the respective corrections, which correspond to the changes in the electrostatic energy of electrons due to the emission of an X-ray quantum and φ_M is the Madelung constant.

Since for transition d elements $Q = Q_{ns} + Q_{(n-1)d} + Q_{np}$ and Q_{np} is small and remains virtually constant on going from one compound to another (see, *e.g.*, the data of EH calculations for Tc compounds in Table 2), it can be neglected. Then, in the general case, δE and ΔE can be represented as functions of $Q_{5s} + Q_{4d}$. The experimental dependences of δE and ΔE on $Q_{5s} + Q_{4d}$ (obtained from EH calculations) have been reported.[77] It has been shown that the dependence $\Delta E = f(Q_{5s} + Q_{4d})$ is close to a linear one, whereas the dependence $\delta E = \varphi(Q_{5s} + Q_{4d})$ is less unambiguous. The values of the coefficients C_{5s}, C_{4d}, δ_{5s}, δ_{4s} and $\delta_{5s,4d}$ were determined after substituting the $Q_{5s} + Q_{4d}$ values taken from EH calculations into Eqn (1) and solving the system of five linear equations with five unknowns.[77] To reduce systematic errors due to inaccuracy in the parametrisation, the data calculated only for the chloride compounds $[TcCl_6]^{2-}$, $[Tc_2Cl_8]^{3-}$, $[Tc_2Cl_8]^{2-}$, $[Tc_2Cl_6]^{2-}$ and $[Tc_6Cl_{12}]^{2-}$ were used.[77] For comparison, analogous coefficients[77] calculated by the Hartree–Fock SCF method for the isolated Tc atoms in the approximation of two alternative configurations ($4d^6 5s^1$ and $4d^5 5s^2$) have also been used. It has been shown that, at least except for sign, the values of all the coefficients in question (C_{5s}, C_{4d}, δ_{5s}, δ_{4d} and $\delta_{5s,4d}$) are close. This indicates indirectly that EH calculations provide a good basis for theoretical description of δE at qualitative and semiquantitative levels.

A one-to-one correspondence between the ΔE and $Q_{5s} + Q_{4d}$ values has been established by extrapolating the $\Delta E = f(Q_{5s} + Q_{4d})$ dependence to all other technetium compounds for which the X-ray emission and X-ray photoelectron spectra have been measured.[77] At this point, it has been assumed that φ_M is independent of $Q_{5s} + Q_{4d}$ or varies monotonically as the latter parameter varies; this has been strictly substantiated only for compounds with similar structure and composition. Then, substituting the $Q_{5s} + Q_{4d}$ value found into Eqn (1) and using the coefficients of this equation calculated in the EH approximation, one could calculate the Q_{5s}, Q_{4d}, and Q_{4p} partial charges (see Table 12). To pass to another, more physically well-founded scale of effective charges, the values of coefficients of Eqn (1) calculated by the Hartree–Fock method were used assuming that Z_{eff} of technetium ($Z_{eff} = q_s + q_d$) in $KTcO_4$ coincides with the effective charge of ruthenium in RuO_4 and is equal to 1.71.[96,97] From the fact that the metal atoms in both d^0 complexes have the same oxygen environment and that the electronegativities of the Tc and Ru atoms are almost equal it follows that these charges are approximately equal.[79,80] Having calculated the partial charges q_s and q_d on technetium atoms in $KTcO_4$ from Eqn (1) and assuming that the found value of the ratio Q_{5s}/q_s (3.57) remains almost constant, it was also possible to calculate[77] the q_s and q_d values for all other technetium compounds for which EH data are available (see Table 12). These calculations have shown that all the experimental results can be described by the following equation:

$$\delta E = (37.5 \pm 2.1) - (156.0 \pm 2.9)(q_s + q_d). \quad (3)$$

Since the correlation coefficient of the linear dependence (3) for nine experimental points is 0.999, it was assumed that δE for all other compounds is also described by this equation. Simultaneous solution of Eqns (1) and (3) performed under this assumption allowed one to find q_s and q_d values for all other technetium compounds. The results obtained[77] are listed in Table 12. The effective charges on the Tc atoms calculated using the two different procedures differ considerably in magnitude. However, all main tendencies and regularities of changes in Z_{eff} on going from one compound to another are the same for both scales of effective charges:[75–77]

1. The Q_{5p} values and their changes for all compounds are small, which indicates that the extent of participation of the 5*p* AO in the formation of chemical bonds is small. The $Q_{5s}(q_s)$ and $Q_{4d}(q_d)$ values decrease regularly as the formal oxidation state of technetium decreases, which points to increasing covalency of chemical bonds in this series of compounds.

2. A tendency for Z_{eff} to increase with increase in the Tc oxidation state, total electronegativity of ligands in the series F > O > Cl > Br > S ≈ I and the polarising capacity of cations Z_{cat}/R_{cat} is observed for compounds containing no M–M bonds.

3. A 'loss of sensitivity' of Z_{eff} to the electronegativity of ligands, the nature of cation and the formal oxidation state of technetium with increase in the number of electrons participating in the formation of M–M bonds is observed for compounds with M–M bonds. In some cases the Z_{eff} value in technetium clusters changes upon insignificant change in the formal oxidation state of Tc or in the structure of the cluster (see, *e.g.*, compounds **41** and **42**, **43** and **44**, **1** and **3**, **5′** and **5″**, and **25** and **3′** in Table 12).

The partial charges of ligands in technetium compounds (Table 13) have been determined from the analysis of q_{s+d} values, comparison of these values with $Z_{eff}(Ru)$[96,97] and using the dependence of q_{s+d} on Z_{EH} for the ligands.[77]

The algebraic sums of charges on all atoms in Tc compounds have been calculated from the data in Tables 12 and 13.[77] These

Table 13. Partial charges on ligands and cations in technetium compounds.[77]

Ligand, cation	Charge	Ligand	Charge	Ligand	Charge
Inorganic cation	+0.82	Cl_{ax}	−0.45	Br_{eq} (clusters)	−0.34
Bulky organic cation	+0.87	Cl_{eq}	−0.36	Br_{bridge}	−0.13
		Cl_{eq} (clusters)	−0.40	I_{ax}	−0.29
F_{eq}	−0.46	Cl_{bridge}	−0.16	S	−0.22(10)
O_{eq} {oxides, $[TcOX_4]^-$}	−0.30(15)	Br_{ax}	−0.37	C	−0.33
O_{eq} $\{[TcO_4]^-\}$	−0.64(1)	Br_{eq}	−0.32	CO	−0.03

Note. The last significant figures of the maximum deviations from average charge values are given in parentheses.

sums differ considerably from zero for binary compounds, which is probably associated with great differences in the nature of ligand bonding with technetium (apparently, one cannot use the same q_{s+d} value for the ligands in all these compounds). Systematic deviations of the sums of charges from zero are observed for compounds with M−M bonds (di- and polynuclear clusters). *A priori* this may be due either to the same reasons as for binary compounds or to systematic changes (as a rule, a decrease) in Z_{eff} of the Tc atoms caused by the M−M bonds. The latter assumption seems to be more reasonable, since X-ray photoelectron spectra of technetium compounds indicate that Z_{eff} of halide ligands of the same structural type are constant irrespective of the presence of M−M bonds in the compounds[67,69,81] (see Section IV).

The averaged deviations of Σq_{s+d} from zero calculated per two Tc atoms using the above procedure for di- and polynuclear clusters of different structural types are equal to −0.22 (dinuclear d^4-d^4 clusters), −0.44 (dinuclear d^4-d^5 clusters), −0.80 (dinuclear d^5-d^5 clusters), −0.53 (trigonal-prismatic clusters) and −0.17 (tetragonal-prismatic clusters).[77]

As can be seen, the decrease in Z_{eff} due to the formation of M−M bonds is a maximum in the case of dinuclear d^5-d^5 clusters. This correlates with the shortest M−M distance (2.04 Å) in their molecules.[57] The influence of relatively long M−M bonds (~ 2.6 Å)[2] on the Z_{eff} value is minimal. It is likely that the effect of multiple M−M bonds in polynuclear prismatic clusters is more pronounced than, *e.g.*, in d^4-d^4 complexes, owing to the additional contribution from several weaker M−M bonds.

Thus, the results obtained[75–77] confirm again that the formation of M−M bonds may cause changes in the effective charges on the metal atoms.[3,51,70–73,87,88] We believe that this phenomenon is due to the specific effect of the system of M−M bonds on the electronic structure of clusters. Therefore, the M−M bonds in technetium clusters (as well as in a number of clusters of other elements) can be considered as specific additional ligands affecting Z_{eff} on the metal core atoms of the clusters.

Later, another approach to the interpretation of the data on chemical shifts in the $K_{\alpha1,2}$ and $K_{\beta1,3}$ lines in X-ray emission spectra of molybdenum, technetium and ruthenium compounds was proposed.[75–77] These results were generalised by Batrakov *et al.*[98] who have analysed two independent sets of experimental parameters corresponding to $\delta K_{\alpha1,2}$ and $\delta K_{\beta1,3}$ in contrast to the chemical shifts for technetium compounds that we have considered previously. However, a considerable increase in the number of parameters directly determined in the experiments does not allow one to interpret the experimental results unambiguously. Thus, *e.g.*, Batrakov *et al.*[98] had to make some assumptions on the electron configuration of the reference compound (TcO_2 in the ionic state 1+ or 3+ has been used as reference compound for technetium compounds). However, from the above discussion it follows that it is just technetium dioxide that can scarcely be used as reference compound, because some of its electronic properties make it different from most other technetium compounds (see also Section IV, Tables 9 and 12 and Figs 9 and 12). Moreover, our calculations performed using a representative random sample of experimental $\delta K_{\alpha1,2}$ and $\delta K_{\beta1,3}$ values taken from Ref. 98 and the approach described above in this Section showed that the final conclusions do not differ fundamentally from those drawn in Ref. 77. In this connection it is not expedient to consider the data and, especially, the interpretation of results obtained by Batrakov *et al.*[98] in detail. We will restrict ourselves to major conclusions only.

The diagram of the chemical shifts of the centres of gravity of the Tc $K_{\alpha1,2}$ and Tc $K_{\beta1,3}$ doublets for technetium compounds (see Ref. 98) is shown in Fig. 13. As can be seen, in the coordinate system used all experimental points fall on five curves corresponding to different types of technetium compounds, *viz.*, oxides, iodides, bromides, chlorides and clusters (including metallic technetium). It should be noted that similar dependences have been obtained for technetium compounds[98] in the coordinates of partial charges Q_{4d} and Q_{5s} which were determined using the approach described above. It was confirmed that the formation of M−M bonds (M = Tc, Mo) results in changes in the effective charges on the atoms of these metals, which is also an important result of this study.

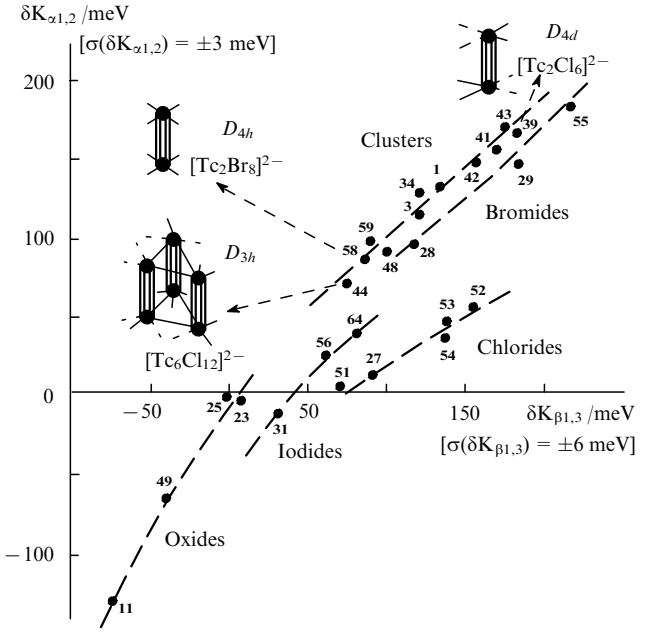


Figure 13. Diagram of the chemical shifts of the centres of gravity of the Tc $K_{\alpha1,2}$ and Tc $K_{\beta1,3}$ doublets in the X-ray emission spectra for technetium compounds according to Batrakov *et al.*[98] The numbering of points corresponds to those of compounds in Tables 9 and 12; the point No. **64** corresponds to $(Me_4N)_2[TcI_6]$).

VI. Compounds with ferrocenium cations

Considering various methods of investigation of technetium clusters, we shall dwell on the ^{57}Fe Mössbauer spectroscopy of ferrocenium-containing complexes. Table 14 presents the parameters of the ^{57}Fe Mössbauer spectra of compounds with ferrocenium cations. As can be seen, the parameters of the Mössbauer spectra depend strongly on temperature and the chemical nature of the anion. At room temperature, doublet (singlet for two compounds) spectra are observed; the chemical shifts δ in the

Table 14. Parameters of ^{57}Fe Mössbauer spectra (δ, Δ, Γ / mm s^{-1}) of compounds with ferrocenium cations.[28, 29]

Compound	T /K	δ	Δ	Γ	Notes
$(FeCp_2)[TcO_4]$	300	0.65	0.74	0.54	doublet
	300 [a]	0.61	0.70	0.60	"
	78	0.75	0.65	0.69	"
	5	0.73	0	1.68	broad singlet
$(FeCp_2)_4[H_3O(H_2O)_4]_2[TcCl_6]_3$	300	0.66	0.14	0.36	doublet
	300 [a]	0.62	0	0.60	singlet
	78	0.74 (*A*)	0.18	0.38	two doublets in the ratio
	78	0.66 (*B*)	0.55	0.37	*A* : *B* = ~7.6 : 1.0
	5	0.80 (*A*)	0	0.53	singlet and doublet in the ratio
	5	0.86 (*B*)	2.37	0.25	*A* : *B* = ~6.6 : 1.0
$(FeCp_2)_3[Tc_6Cl_{14}]$	300	0.66	0	0.50	singlet
	78	0.65 (*A*)	0	0.60	singlet and two doublets in the ratio
	78	0.80 (*B*)	2.30	0.40	*A* : *B* : *C* = ~2.3 : 1.0 : 1.0
	78	0.70 (*C*)	0.30	0.50	
$(FeCp)_2[Tc_8Br_{14}]$	300	0.70	0	0.45	singlet
	78	0.62 (*A*)	0	0.60	singlet and two doublets in the ratio
	78	0.83 (*B*)	2.35	0.60	*A* : *B* : *C* = ~2.0 : 1.0 : 1.0
	78	0.72 (*C*)	0.35	0.42	
$(FeCp_2)_2[Tc_6I_{14}]$	300	0.68	0.44	0.47	doublet
	300 [b]	0.68	0.46	0.48	"
	78	0.78	0.46	0.53	"
$(FeCp_2)_2[Re_2Br_8]$	300	0.62	0.68	0.59	"
	300 [b]	0.62	0.71	0.67	"
	78	0.72	0.64	0.65	"
$(FeCp_2)_2PF_6$	300	0.66	0.30	0.31	"
	78	0.77	0.30	0.30	"
$FeCp_2$	300	0.60	2.37	0.24	"
	78	0.76	2.38	0.30	"

[a] The specimen was preliminarily frozen to 5 K. [b] The specimen was preliminarily frozen to 78 K.

spectra depend slightly on the nature of the anion and the quadrupole splitting Δ decreases for the anions in the series: $[TcO_4]^- > [Re_2Br_8]^{2-} > [Tc_6I_{14}]^{3-} > [PF_6]^{2-} > [TcCl_6]^{2-} > [Tc_6Cl_{14}]^{3-} \approx [Tc_8Br_{14}]^{2-}$. Spectral line broadening is observed as the temperature decreases. Additional lines appear in the spectra of compounds with the $[TcCl_6]^{2-}$, $[Tc_6Cl_{14}]^{3-}$ and $[Tc_8Br_{14}]^{2-}$ anions; the parameters of one of these lines are close to those of the Fe^{2+} signal in pure ferrocene [30] (see Table 14 and Fig. 14). For cluster anions, this is observed even at 78 K, whereas for ferrocenium hexachlorotechnetate(IV) this is observed only at 5 K (at 78 K, the spectrum of this compound is appreciably broadened and can be deconvoluted into two doublets with small Δ by the least squares method assuming a Lorentzian lineshape). The spectrum of ferrocenium pertechnetate at 5 K is a broad singlet; however, attempts at its deconvoluting into components failed.

Physicochemical studies [28, 29] of compounds with ferrocenium cations (see also Sections II–IV) allow one to draw the following principal conclusions:

1. All compounds possess anomalous peculiarities of electronic structure due to the changes in their physicochemical properties with time and temperature.

2. Anomalous properties increase for the series of anions as follows: $[TcO_4]^- \approx [Re_2Br_8]^{2-} \approx [Tc_6I_{14}]^{3-} < [TcCl_6]^{2-} < [Tc_6Cl_{14}]^{3-} < [Tc_8Br_{14}]^{2-}$.

The following explanation of this anomaly was proposed.[28, 29] It was shown[64] that the probability of participation of outer *ns* (*np*) technetium (rhenium) AOs in the formation of coordinate bonds formed by this atom increases in the above series of anions (except for the iodide cluster). This is due to the fact that the 4*d* AOs become destabilised to a greater extent than diffuse 5*s* (5*p*) AOs capable of effective interaction at comparatively long distances (> 2.5 Å) as the formal oxidation state of technetium (the effective charge on its atoms) decreases. There are also low-lying MOs formed by diffuse 4*s* (4*p*) orbitals of Fe atoms in ferrocenium cations.[99] An approach of Fe and Tc atoms within a distance of ~ 5 Å (it is this distance that is observed in ferrocenium complexes of technetium) must result in direct electron overlap of *ns* (*np*) orbitals of the Fe and Tc atoms and, hence, in the formation of conduction bands. Indeed, all compounds possess temperature-independent semiconductor-type conductivity. This indicates that the Fermi levels of the ferrocenium cations and technetium (rhenium) anions in these compounds are inside or near the *sp* conduction bands. This may result in tunnelling of the valence *sp* electrons between the anions and cations at frequency ω. Such a dynamic electron transfer along the anion–cation chains can be detected using only those physical methods that have a better time resolution than the average lifetime of the valence electron in the proximity of the atom under observation. In other words, these changes can be detected using photoelectron spectroscopy with a time resolution (τ) of 10^{-16}–10^{-17} s, whereas only an averaged picture can be obtained using such integral methods as static magnetic susceptibility, heat capacity and conductivity measurements, X-ray analysis, *etc*. The results obtained by Mössbauer, EPR, and IR spectroscopy with a time resolution of 10^{-7} s, ~ 10^{-9}–10^{-10} s and 10^{-11}–10^{-13} s, respectively, will be intermediate due to line broadening in spectra caused by dynamic electron transfer and vibronic interaction.

In the context of the proposed explanation of the properties of compounds with ferrocenium cations,[28, 29] attention must be focused on the magnetic properties (see Sections III and IV) and changes in the photoelectron spectra of these compounds at low

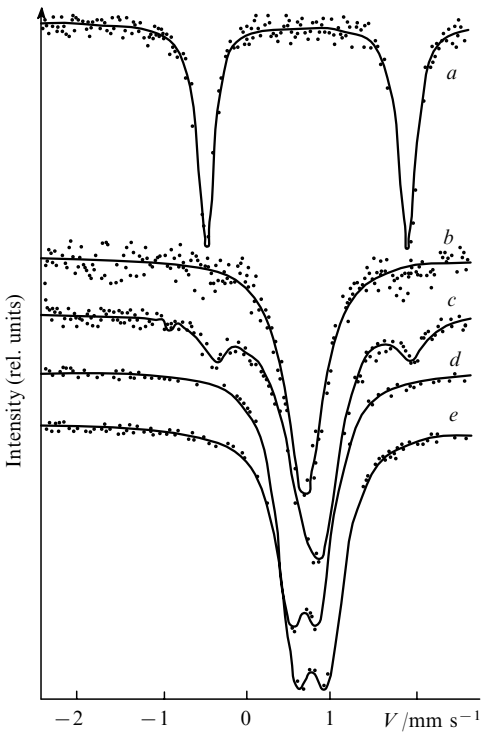


Figure 14. ^{57}Fe Mössbauer spectra of: (*a*) $FeCp_2$ at 300 K; (*b*, *c*) $(FeCp_2)_3 \cdot \{[Tc_6Cl_6(\mu\text{-}Cl)_6]Cl_2\}$ at 300 and 80 K; (*d*, *e*) $(FeCp_2)_2[PF_6]$ at 300 and 80 K.

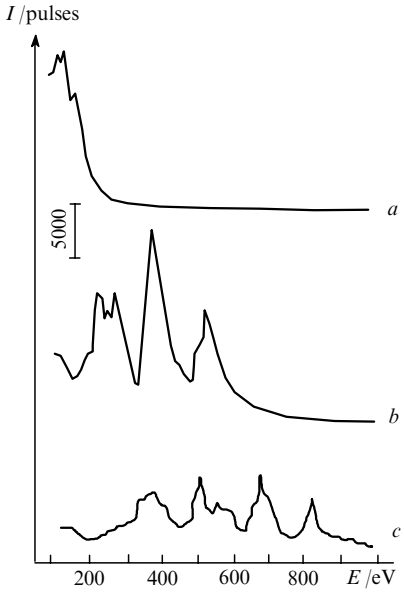


Figure 15. Dynamics of anomalous electron emission for a $(FeCp_2)_2[Tc_8Br_{14}]$ specimen preliminarily cooled to ~ 100 K after switching on the X-ray radiation source (at a beam power of 200 W) during data collection (1000 eV/256 channels) in one scan (data collecting time of 210 s). Start of data collection after switching on the X-ray radiation source: (*a*) 0 min; (*b*) 4 min.; and (*c*) 8 min. (Here *E* is the kinetic energy of electrons).[28,29]

temperatures. Thus, Table 9 presents the experimental parameters of X-ray photoelectron spectra of several technetium and rhenium compounds (see also Refs 28 and 29). From these data it follows that the X-ray photoelectron spectra of the compounds with ferrocenium cations recorded at room temperature for the first time do not differ fundamentally from those of other technetium and rhenium compounds. All major spectral regularities correspond to those described above (see Sections IV.1–IV.3). The only exception is the increased binding energy corresponding to the Tc 3*d* line in the case of $(FeCp_2)_2[Tc_8Br_{14}]$. However, anomalous electron emission is observed at a temperature of about 100 K instead of conventional X-ray photoelectron spectra of the compounds with ferrocenium cations and $[TcCl_6]^{2-}$, $[Tc_6Cl_{14}]^{3-}$ and $[Tc_8Br_{14}]^{2-}$ anions. No temperature dependence of spectra of other compounds has been found.

The phenomenon of anomalous electron emission consists in the following.[28,29] The lines of the conventional X-ray photoelectron spectrum (Fig. 15) become diffuse and disappear as the temperature of the specimens decreases below a specific threshold value (~ 100 K). The spectrum of inelastic electrons observed simultaneously with the lines of the X-ray photoelectron spectrum loses its true shape and also disappears against the background of a group of very intense lines; the structure and number of these lines vary substantially on fast freezing of the specimen. The amplitudes of the most intense peaks are approximately 2 orders of magnitude larger than the intensities of the lines in the conventional X-ray photoelectron spectrum, which usually results in overloading of the detector even at the minimum power of the X-ray radiation source (100 W for an HP 5950A spectrometer). Further cooling of the specimens leads to substantial increase in the upper boundary kinetic energy (UBKE) of emitted electrons (from 10 to $\geqslant$ 1500 eV). The UBKE changes analogously with the increase in duration of exposure of the specimens in which approximate temperature equilibrium was reached to X-ray radiation. The UBKE decreases slowly until the anomalous emission ceases and the conventional X-ray photoelectron spectrum recovers as the specimens undergo slow unfreezing. The qualitative and quantitative spectral pattern is reproduced within short time intervals (~ 5 min) under conditions of relative stabilisation of the specimen temperature. To a first approximation, the intensities of the peaks were found to be proportional to the power of the X-ray tube of the spectrometer. With an accuracy of ~ 0.1 s, no time lag was found on switching off the X-ray tube. The kinetic energy of emitted electrons can exceed the energy of exciting X-ray quanta (1486.6 eV).

The second peculiarity of the X-ray photoelectron spectra of compounds with ferrocenium cations is that the spectra recorded repeatedly at room temperature (after freezing of the specimens to 78 K followed by their unfreezing) can differ from those recorded initially at the same temperature. These differences include[28,29] the following features: (1) the peaks corresponding to the core electrons of the Fe atoms correspond in the repeatedly recorded spectra to three nonequivalent states of these atoms {compounds with $[Tc_6Cl_{14}]^{2-}$ and $[Tc_8Br_{14}]^{2-}$ anions} and (2) the same holds for the peaks corresponding to the core electrons of the halogen atoms {the compound with the $[TcCl_6]^{2-}$ anion}. These data could indicate that the compounds with ferrocenium cations are initially in the metastable state and are stabilised on freezing. However, the temperature dependences of the heat capacity and the magnetic susceptibility of the compounds studied show that no phase transitions occur in the temperature range from 300 to 100 K. Thus, the effects observed are due to pure electronic peculiarities of the structure of the compounds under consideration. It should be noted that the Mössbauer and IR spectra (see Sections II and VI, respectively) of the specimens that were preliminarily frozen repeatedly recorded at room temperature also differ somewhat from those recorded initially.¶

Phenomena similar to that observed[28,29] are known: exoelectron emission (see, *e.g.*, Ref. 100) and mechanoemission.[101] It is likely that the charges accumulated in the specimen subjected to X-ray radiation are to a great extent responsible for the appear-

¶ Changes in the specimens caused by freezing cannot be due to any chemical processes, since the specimens are stable towards water sorption on the surface; no changes in the chemical composition were found.[28,29]

ance of anomalous electron emission.[78] The peculiarities of the low-temperature X-ray photoelectron spectra of some compounds with ferrocenium cations observed in the experiments may be due to the multiphoton photoeffect similar to the laser effect.[28, 29]

As has been mentioned in Section III, the magnetic properties of compounds with ferrocenium cations are also anomalous. In fact, as can be seen from the data in Table 8, in all cases there is more than one unpaired electron per ferrocenium cation. It is obvious that the effective number of unpaired electrons may be increased due to the partial unpairing of the occupied cationic and anionic MOs composed mainly of *ns* (*np*) AOs and forming the conduction bands. The effective number of unpaired electrons may also change appreciably due to the changes in the vibronic interaction caused by temperature changes. In this case the paramagnetism of the compound will be the sum of the contributions of *d* electrons of the cations and anions and *s* electrons of the conduction band. Because of the fast dynamic electron transfer (the $s-d-s$ exchange), the lines in the EPR spectra of the compounds will be appreciably broadened or unobservable {as in the case of compound with the $[Tc_8Br_{14}]^{2-}$ anion}. The central, more narrow component of the EPR spectra will correspond mainly to *d* electrons of cations and anions, whereas the broader component will correspond to the electrons of the *s* conduction band.

VII. Conclusion

The experimental and theoretical substantiation of the participation of the outer $5s$ ($5p_z$) orbitals of the Tc atoms in the formation of bonding 'metallic' MOs in technetium clusters with the formal oxidation state of Tc no more than 2.0 is presented in this review. On the one hand, this effect results in strengthening of the M—M bonding in technetium clusters containing a formally 'excess' number of 'metallic' electrons (*i.e.*, the number exceeding that corresponding to the closed shell of the bonding MOs composed of $4d$ AOs). On the other hand, it enhances shielding of the positive nuclear charges (a decrease in Z_{eff}) of the Tc atoms in technetium clusters, thus decreasing the Coulomb repulsion in the formation of M—M bonds and increasing the contribution of electron correlation effects to the ground electronic state of the system. Thus, it also leads to an increase in the cluster-forming properties of technetium. This theoretical substantiation agrees well with the descriptions of the 'anomalous' properties of technetium clusters reported earlier.[3, 51]

This review has been written with partial financial support of the Russian Foundation for Basic Research (Project No. 96-03-33125a/240).

References

1. F A Cotton, R Walton *Multiple Metal–Metal Bonds* (New York: Wiley, 1982)
2. S V Kryutchkov *Top. Curr. Chem.* **176** 189 (1996)
3. S V Kryutchkov *Koord. Khim.* **11** 637 (1985) [a]
4. S V Kryutchkov, Candidate Thesis in Chemical Sciences, Institute of Physical Chemistry, Academy of Sciences of the USSR, Moscow, 1983
5. W Preetz, G Z Peters *Z. Naturforsch., B Chem. Sci.* **35** 797 (1980)
6. W Preetz, G Peters, D Bublitz *J. Cluster Sci.* **5** 83 (1994)
7. L L Zaitseva, A S Kotel'nikova, A A Rezvov *Zh. Neorg. Khim.* **25** 2624 (1980) [b]
8. F A Cotton, P E Fanwick, L D Gage, B Kalbacher, D S Martin *J. Am. Chem. Soc.* **99** 5642 (1977)
9. F A Cotton, B Kalbacher *Inorg. Chem.* **16** 2386(1977)
10. F A Cotton, P E Fanwick, L D Gage *J. Am. Chem. Soc.* **102** 1570 (1980)
11. V I Spitsyn, A F Kuzina, S V Kryutchkov *Zh. Neorg. Khim.* **25** 741 (1980) [b]
12. H B Burgi, G Anderegg, P Blauenstein *Inorg. Chem.* **20** 3829 (1981)
13. G Anderegg, E Miller, K Zollinger, H B Burgi *Helv. Chim. Acta* **66** 1593 (1983)
14. K E Linder, J C Dewan, A Davison *Inorg. Chem.* **20** 3820 (1981)
15. S V Kryutchkov, A E Simonov *Izv. Akad. Nauk SSSR, Ser. Khim.* 2140 (1987) [c]
16. S V Kryutchkov, A E Simonov *Koord. Khim.* **16** 339 (1990) [a]
17. S V Kryutchkov, A F Kuzina, V I Spitsyn *Zh. Neorg. Khim.* **28** 1984 (1983) [b]
18. S V Kryutchkov, Candidate Thesis in Chemical Sciences, Institute of Physical Chemistry, Russian Academy of Sciences, Moscow, 1991
19. S V Kryutchkov, A F Kuzina, V I Spitzin *Z. Anorg. Allg. Chem.* **563** 153 (1988)
20. P A Koz'min, T B Larina, M D Surazhskaya *Dokl. Akad. Nauk SSSR* **271** 1157 (1983) [d]
21. V I Spitsyn, B Baierl, S V Kryutchkov, A F Kuzina, M Varen *Dokl. Akad. Nauk SSSR* **256** 608 (1981) [d]
22. P A Koz'min, T B Larina, M D Surazhskaya *Koord. Khim.* **7** 1719 (1981) [a]
23. P A Koz'min, T B Larina, M D Surazhskaya *Koord. Khim.* **8** 851 (1982) [a]
24. P A Koz'min, T B Larina, M D Surazhskaya *Koord. Khim.* **9** 1114 (1983) [a]
25. A I Grigor'ev, in *Vvedenie v Kolebatel'nuyu Spektroskopiyu Neorganicheskikh Soedinenii* (Introduction in Vibrational Spectroscopy of Inorganic Compounds) (Moscow: Moscow Sate University, 1977) p. 31
26. P A Koz'min, M D Surazhskaya *Koord. Khim.* **6** 653 (1980) [a]
27. F A Cotton, B A Frenz, W Shive *Inorg. Chem.* **14** 649 (1975)
28. B G Antipov, S V Kryutchkov, V N Gerasimov, M S Grigoriev, P E Kazin, V V Kharitonov , V G Maksimov, V S Moisa, V V Sergeev, T K Yurik *Radiochim. Acta* **64** 191 (1994)
29. B G Antipov, S V Kryutchkov, V N Gerasimov, M S Grigor'ev, P E Kazin, V V Kharitonov, V G Maksimov, S V Moisa, V V Sergeev, T K Yurik *Koord. Khim.* **21** 716 (1995) [a]
30. V T Aleksanyan, B V Lokshin, in *Stroenie Molekul i Khimicheskaya Svyaz' (Itogi Nauki i Tekhniki)* [The Structure of Molecules and Chemical Bond (Advances in Science and Engineering Series)] (Moscow: Izd. VINITI, 1976) Vol. 5
31. S V Kryutchkov, M S Grigoriev, K E German, in *Technetium and Rhenium in Chemistry and Nuclear Medicine* Vol. 3 (Eds M Nicolini, G Bandoly, U Mazzi) (New York: Raven Press, 1990) p. 253
32. K Schwochau, K Hedwig, H J Schenk *Inorg. Nucl. Chem. Lett.* **13** 77 (1977)
33. V T Kalinnikov, Yu V Rakitin *Vvedenie v Magnetokhimiyu. Metod Staticheskoi Magnitnoi Vospriimchivosti* (Introduction in Magnetochemistry. The Method of Static Magnetic Susceptibility) (Moscow: Nauka, 1980)
34. S V Kryutchkov, Yu V Rakitin, P E Kazin, A I Zhirov, N Yu Konstantinov *Koord. Khim.* **16** 1230 (1990) [a]
35. V I Spitsyn, A F Kuzina *Tekhnetsii* (Technetium) (Moscow: Nauka, 1981)
36. L L Zaitseva, A V Velichko, I V Vinogradov *Neorganicheskaya Khimiya (Itogi Nauki i Tekhniki)* [Inorganic Chemistry (Advances in Science and Engineering Series)] (Moscow: Izd. VINITI, 1984) Vol. 9
37. V P Tarasov, S A Petrushin, V I Privalov, K E German, S V Kryutchkov, Yu A Buslaev *Koord. Khim.* **12** 1227 (1986) [a]
38. V P Tarasov, V I Privalov, S A Petrushin, G A Kirakosyan, K E German, S V Kryutchkov, Yu A Buslaev *Dokl. Akad. Nauk SSSR* **272** 919 (1983) [d]
39. V P Tarasov, S A Petrushin, G A Kirakosyan, K E German, S V Kryutchkov, in *Spektroskopiya Koordinatsionnykh Soedinenii (Tez. Dokl. III Vsesoyuz. Soveshch.), Krasnodar, 1984* [Spectroscopy of Coordination Compounds (Abstracts of Reports of the Third All-Union Meeting), Krasnodar,1984] p. 82
40. V P Tarasov, V I Privalov, K E German, S V Kryutchkov *J. Nucl. Medicine*. **33** 319 (1989)
41. V P Tarasov, V I Privalov, K E German, S V Kryutchkov, in *Technetium and Rhenium in Chemistry and Nuclear Medicine* Vol. 3 (Eds M Nicolini, G Bandoly, U Mazzi) (New York: Raven Press, 1990) p. 321
42. K E German, M S Grigor'ev, A F Kuzina, V I Spitsyn *Zh. Neorg. Khim.* **32** 1089 (1987) [b]

43. K E German, M S Grigor'ev, A F Kuzina, B F Gulev, V I Spitsyn *Dokl. Akad. Nauk SSSR* **287** 650 (1986) [d]
44. V I Spitsyn, A F Kuzina, K E German, M S Grigor'ev *Dokl. Akad. Nauk SSSR* **293** 101 (1987) [d]
45. L Astheimer, K Schwochau *J. Inorg. Nucl. Chem.* **38** 1131 (1976)
46. L Astheimer, J Hauck, H J Schenk, K Schwochau *J. Chem. Phys.* **63** 1988 (1975)
47. F A Cotton, A Davison, V W Day, L D Gage, H S Trop *Inorg. Chem.* **18** 3024 (1979)
48. V I Spitsyn, A I Zhirov, M Yu Subbotina, P A Kazin *Zh. Neorg. Khim.* **25** 998 (1980) [b]
49. S V Kryutchkov, M S Grigor'ev *Koord. Khim.* **15** 1343 (1989) [a]
50. A Magneli, G Andersson *Acta Chem. Scand.* **9** 1378 (1955)
51. V I Spitsyn, A F Kuzina, A A Oblova, S V Kryutchkov *Usp. Khim.* **54** 637 (1985) [*Russ. Chem. Rev.* **54** 373 (1985)]
52. Yu V Rakitin, V I Nefedov *Zh. Neorg. Khim.* **29** 510 (1985) [b]
53. F A Cotton, E Pedersen *Inorg. Chem.* **14** 383 (1975)
54. Yu V Rakitin, S V Kryutchkov, A I Aleksandrov, A F Kuzina, N V Nemtsev, B G Ershov, V I Spitsyn *Dokl. Akad. Nauk SSSR* **269** 1123 (1983) [d]
55. A Abraham, B Blini *Electron Paramagnetic Resonance of Transition Ions* Vol. 1 (Oxford: Clarendon Press, 1970)
56. S A Al'tshuler, B M Kozyrev *Elektronnyi Paramagnitnyi Rezonans Soedinenii Elementov Promezhutochnykh Grupp* (Electron Paramagnetic Resonance of Compounds of Elements of Intermediate Groups) (Moscow: Nauka, 1972) p. 69
57. S V Kryutchkov, M S Grigor'ev, A F Kuzina, B F Gulev, V I Spitsyn *Dokl. Akad. Nauk SSSR* **288** 389 (1986) [d]
58. F A Cotton, L M Daniels, L R Falvello, M S Grigoriev, S V Kryutchkov *Inorg. Chim. Acta* **189** 53 (1991)
59. P A Agaskar, F A Cotton, K R Dunbar, L R Falvello, S M Tetrick, R A Walton *J. Am. Chem. Soc.* **108** 4850 (1986)
60. P A Koz'min, T B Larina, M D Surazhskaya *Koord. Khim.* **13** 415 (1987) [a]
61. S V Kryutchkov, M S Grigor'ev, A F Kuzina, B F Gulev, V I Spitsyn *Dokl. Akad. Nauk SSSR* **288** 893 (1986) [d]
62. R Wheeler, R Hoffmann *J. Am. Chem. Soc.* **108** 6605 (1986)
63. R Wheeler, R Hoffmann *Angew. Chem., Int. Ed. Engl.* **25** 822 (1986)
64. S V Kryutchkov, V S Mironov, B G Antipov, Yu V Plekhanov *Metalloorg. Khim.* **4** 52 (1991) [e]
65. Yu L Slovokhotov, Yu T Struchkov *Usp. Khim.* **54** 556 (1985) [*Russ. Chem. Rev.* **54** 323 (1985)
66. S P Gubin *Khimiya Klasterov. Osnovy Klassifikatsii i Stroenie* (The Chemistry of Clusters. Classification and Structure) (Moscow: Nauka, 1987)
67. V I Spitzin, S V Kryutchkov, M S Grigoriev, A F Kuzina *Z. Anorg. Allg. Chem.* **563** 136 (1988)
68. S V Kryutchkov, A F Kuzina, V I Spitsyn *Dokl. Akad. Nauk SSSR* **287** 1400 (1986) [d]
69. F A Cotton, L M Daniels, L R Falvello, M S Grigoriev, S V Kryutchkov *Inorg. Chim. Acta* **189** 53 (1991)
70. V N Gerasimov, S V Kryutchkov, A F Kuzina, V M Kulakov, S V Pirozhkov, V I Spitsyn *Dokl. Akad. Nauk SSSR* **266** 148 (1982) [d]
71. V N Gerasimov, S V Kryutchkov, K E German, V M Kulakov, A F Kuzina. *J. Nucl. Medicine* **33** 285 (1989)
72. V N Gerasimov, S V Kryutchkov, K E German, V M Kulakov, A F Kuzina, in *Technetium and Rhenium in Chemistry and Nuclear Medicine* Vol. 3 (Eds M Nicolini, G Bandoly, U Mazzi) (New York: Raven Press, 1990) p. 231
73. V N Gerasimov, S V Kryutchkov, K E German, V M Kulakov, A F Kuzina *Rentgenoelektronnoe Issledovanie Stroeniya Kompleksnykh Soedinenii Tekhnetsiya (Preprint IAE-5041/9)* [X-Ray Electron Spectroscopy Study of the Structure of Complex Compounds of Technetium (Preprint INP-5041/9)] (Moscow: I V Kurchatov Institute of Nuclear Power, 1990)
74. V N Gerasimov, A F Kuzina, V M Kulakov, S V Kryutchkov, in *Tez. Dokl. IV Seminara Spetsialistov Sots. Stran po Elektronnoi Spektroskopii* (Abstracts of Reports of the Fourth Seminar of Specialists from Socialistic Countries on Electronic Spectroscopy) (Moscow: Institute of Organic and Inorganic Chemistry, Academy of Sciences of the USSR, 1982) p. 22
75. L L Makarov, S V Kryutchkov, N O Sablina, Yu M Zaitsev, K E German, A F Kuzina, V I Spitsyn *Dokl. Akad. Nauk SSSR* **307** 644 (1989) [d]
76. L L Makarov, S V Kryutchkov, Yu M Zaytsev, N O Sablina, K E German, A F Kuzina *J. Nuclear Medicine* **33** 301 (1989)
77. L L Makarov, S V Kryutchkov, Yu M Zaytsev, N O Sablina, K E German, A F Kuzina, in *Technetium and Rhenium in Chemistry and Nuclear Medicine* Vol. 3 (Eds M Nicolini, G Bandoly, U Mazzi) (New York: Raven Press, 1990) p. 265
78. V I Nefedov *Rentgenoelektronnaya Spektroskopiya Khimicheskikh Soedinenii. Spravochnik* (X-Ray Electron Spectroscopy of Complex Compounds. Handbook) (Moscow: Khimiya, 1984)
79. S S Batsanov *Elektrootritsatel'nost' i Effektivnye Zaryady Atomov* (Electronegativity and Effective Charges of Atoms) (Moscow: Znanie, 1971)
80. S S Batsanov *Strukturnaya Refraktometriya* (Structural Refractometry) (Moscow: Vysshaya Shkola, 1976)
81. A Katrib, R M Yousef, N J Fitzpatrick *Inorg. Chem.* **21** 1523 (1982)
82. S A Best, R A Walton *Inorg. Chem.* **18** 484 (1979)
83. D G Tisley, R A Walton *J. Mol. Struct.* **17** 401 (1973)
84. V I Nefedov, Ya V Salyn *J. Electr. Spectr.* **16** 299 (1979)
85. V I Nefedov, Ya V Salyn, A V Shtemenko, A S Kotelnikova *Inorg. Chim. Acta* **45** L49 (1980)
86. G P Kostikova, Yu P Kostikov, S J Troyanov, D V Korol'kov *Inorg. Chem.* **17** 2279 (1978)
87. G P Kostikova, D V Korol'kov *Usp. Khim.* **54** 591 (1985) [*Russ. Chem. Rev.* **54** 344 (1985)]
88. G P Kostikova, D V Korol'kov *Zh. Vses. Khim. O-va im D I Mendeleeva* **32** 55 (1987) [f]
89. Yu V Plekhanov, S V Kryutchkov *Koord. Khim.* **24** 661 (1998) [a]
90. G Bandoli, U Mazzi, E Roncary, E Deutsch *Coord. Chem. Rev.* **44** 191 (1982)
91. M Melnik, J E Van Lier *Coord. Chem. Rev.* **77** 275 (1987)
92. S V Kryutchkov, M S Grigor'ev, A I Yanovskii, Yu T Struchkov, V I Spitsyn *Dokl. Akad. Nauk SSSR* **301** 618 (1988) [d]
93. E Hartmann, R Der, M Nagel *Z. Phys. A, At Nucli* (*Germany*) **290** 349 (1979)
94. M Benard *J. Am. Chem. Soc.* **100** 2354 (1978)
95. Yu M Zaitsev, Yu F Batrakov, L L Makarov *Teor. Eksp. Khim.* **14** 352 (1978) [g]
96. L L Makarov, A B Nikol'skii, Yu M Zaitsev, Yu F Batrakov, Yu I D'yachenko *Koord. Khim.* **2** 1646 (1976) [a]
97. L L Makarov, A B Nikol'skyi, Ju M Zaitsev, Ju F Batrakov, Ju I Djatchenko, A K Morosov *J. Res. Inst. Catal. Hokkaido Univ.* **24** 102 (1976)
98. Yu F Batrakov, N O Sablina, L L Makarov *Koord. Khim.* **21** 642 (1995) [a]
99. V I Nefedov, V I Vovna *Elektronnaya Struktura Khimicheskikh Soedinenii* (Electronic Structure of Chemical Compounds) (Moscow: Nauka, 1987)
100. N I Kobzev (Ed.) *Ekzoelektronnaya Emissiya* (Exoelectronic Emission) (Moscow: Inostr. Lit., 1962)
101. B V Deryagin, Yu P Toropov, in *XVIII Vsesoyuz. Konf. po Emissionnoi Elektronike (Tez. Dokl.)* [The XVIIIth All-Union Conference on Emission Electronics (Abstracts of Reports)] (Moscow: Nauka, 1981) p. 361

[a] — *Russ. J. Coord. Chem. (Engl. Transl.)*
[b] — *Russ. J. Inorg. Chem. (Engl. Transl.)*
[c] — *Russ. Chem. Bull. (Engl. Transl.)*
[d] — *Dokl. Chem. Technol., Dokl. Chem. (Engl. Transl.)*
[e] — *Organomet. Chem. (Engl. Transl.)*
[f] — *Mendeleev Chem. J. (Engl. Transl.)*
[g] — *Theor. Exp. Chem. (Engl. Transl.)*